LASER-EXCITED IONIC FLUORESCENCE OF THE RARE EARTHS IN THE INDUCTIVELY COUPLED PLASMA

BY

MARIO ELMEN TREMBLAY

A DISSERTATION PRESENTED TO THE GRADUATE SCHOOL
OF THE UNIVERSITY OF FLORIDA IN
PARTIAL FULFILLMENT OF THE REQUIREMENTS
FOR THE DEGREE OF DOCTOR OF PHILOSOPHY

UNIVERSITY OF FLORIDA

1987

To my parents, wife, and daughter,

whose loving support made all this possible.

ACKNOWLEDGMENTS

I wish to thank Dr. James D. Winefordner for the support and guidance he gave me during my graduate career at the University of Florida.

I also wish to thank Dr. Ben Smith and Dr. Ed Voigtman for their guidance and assistance.

Finally, I sincerely thank my parents; my wife, Beverly; and my daughter, Kimberly, for their love and encouragement which made all this possible.

TABLE OF CONTENTS

LIST OF TABLES

LIST OF FIGURES

Abstract of Dissertation Presented to the Graduate School of the University of Florida in Partial Fulfillment of the Requirements for the Degree of Doctor of Philosophy

LASER-EXCITED IONIC FLUORESCENCE OF THE RARE EARTHS IN THE INDUCTIVELY COUPLED PLASMA

BY

MARIO ELMEN TREMBLAY

December, 1987

Chairman: James D. Winefordner
Major Department: Chemistry

Laser excitation of ionic fluorescence overcomes the problem of spectral interferences encountered when doing trace analysis of the rare earths by atomic emission spectrometry in the inductively coupled plasma.

One or two pulsed tunable dye lasers pumped with an excimer laser are used to excite ionic fluorescence of the rare earths in the inductively coupled plasma. Because several fluorescence lines have been observed after laser excitation, it was possible to draw partial energy level diagrams for most of the rare earths. Nonresonance fluorescence lines were used for all measurements in order to minimize spectral interferences. Detection limits at given excitation wavelength are reported for each element. This was the first time that ionic fluorescence

was observed for any of the rare earths in the inductively coupled plasma. Nonresonance as well as resonance fluorescence was detected for all of the rare earths studied except for holmium.

CHAPTER I
INTRODUCTION

Statement of the Purpose

The goal of the research presented in this dissertation is to demonstrate the application of laser-excited ionic fluorescence in the inductively coupled plasma (ICP) to the selective determination of trace level concentration of rare earth (RE) in a mixture of all REs without spectral interferences. This chapter is devoted to an introduction of atomic fluorescence spectrometry (AFS) for trace element analysis with special emphasis on the laser as an excitation source and an ICP as an atom/ion reservoir.

Atomic Fluorescence Spectrometry

Atomic fluorescence in flames was first observed in 1924 by Nichols and Howes (1). However, it was not until 1964 that Winefordner and Vickers (2) first introduced the use of AFS as an analytical method for the measurement of a number of metals. In their approach, the analyte solution is nebulized into a flame where atomization of the analyte takes place. A light source is then directed onto the flame where the absorption of radiation of proper

frequency causes some of the analyte atoms to become excited to an electronic state above the ground state. Some of these excited atoms may return to a lower electronic state through radiational deactivation. This process is also known as atomic fluorescence and is measured at right angles from the incident excitation radiation. The frequency of the light emitted through the fluorescence process is characteristic of the analyte atoms, and the intensity of the signal is related to the concentration of the analyte atoms in the sample. Since then, several reviews (3-5) of AFS have been written in which extensive discussion of previous analytical studies are given.

Excitation Sources

The linear dependence of the atomic fluorescence signal upon the excitation source intensity has led to the development and use of a variety of high intensity line and continuum light sources. The continuum source offers the advantage of providing only one light source for exciting the atomic fluorescence of several elements. However, these sources generally have low spectral irradiance over the spectral region of atomic absorption. Most of the work in AFS has been done with intense line sources which are generally useful for only one or a few elements.

The desirable properties of an ideal excitation source in AFS include short and long term stability; simplicity of use; versatility in terms of wavelength range; and, the most critical of all, high spectral irradiance over the atomic absorption line width. The most common types of AFS sources and comments concerning their use will be discussed.

In 1964, Winefordner and Staab (6) used vapor discharge lamps as line sources for the atomic fluorescence determination of cadmium and zinc. However, because these lamps are characterized by severely broadened and self-reversed spectral line emission, they are not used anymore.

In 1966, Armentrout (7) used hollow cathode lamps (HCLs) for his atomic fluorescence work. Commercially available HCLs are considered to be low intensity line sources. They do not possess sufficient intensity to be of great use in AFS, but it is possible to pulse these lamps momentarily with higher current, thus increasing their intensity. High intensity HCLs are also available. The use of HCLs in AFS has been restricted to a few studies because of their poor spectral irradiance over the absorption line width of an atom.

A new boosted-output HCL is now being investigated by Demers and Skrabak (8) as excitation sources for AFS in the ICP. Boosted-output lamps are basically HCLs in which

an electron emitter has been added in order to improve the efficiency of excitation of the sputtered atoms. These lamps possess the power of an electrodeless discharge lamp (EDL) with the low background noise of a HCL. Because of the improved spectral irradiance and low background noise of the boosted-output HCL, these lamps should become more useful than HCLs for AFS studies.

The xenon arc lamp was first used for atomic fluorescence measurements in 1966 by Veillon, Mansfield, Parsons, and Winefordner (9). Since this type of lamp is a continuum source, it can be used for multi-element analysis. However, the spectral irradiance of xenon arc lamps is low over the atomic absorption line width.

A major breakthrough in AFS occurred in 1966 with the use of electrodeless discharge lamps (EDLs) for excitation sources (10,11). This was the first time that the atomic fluorescence detection limits could compete with atomic emission and atomic absorption method of analysis. In 1967, Dagnall, Thompson, and West (12) were the first to report the measurement of nonresonance atomic fluorescence. By measuring nonresonance fluorescence, it was possible to minimize scattering which was probably the most serious limitation in AFS. From the results obtained in the past, it can be concluded that AFS will continue to improve as long as excitation sources continue to improve. These improvements include more intense light

sources because the fluorescence signal is directly related to the intensity of the excitation radiation and excitation sources which possess narrower spectral bandwidth, since this would minimize the possibility of spectral interferences from other elements. These lamps have higher spectral irradiance than the previous two line sources. The main drawback with EDLs is the lack of commercial availability of good lamps for some elements.

The ICP (13) has recently been used as an excitation source for AFS. The spectral characteristics of the emission from the ICP, such as high intensity, excellent short and long term stability, narrow line width, and freedom from self-reversal of spectral lines, make the ICP an excellent radiation source for AFS. One advantage compared to other AFS excitation source is its flexibility with respect to the availability of intense atomic and ionic lines for many elements. One can change from one element to another by aspirating a solution containing the element of interest into the source ICP.

Finally, in 1971, Fraser and Winefordner (14) and Denton and Malmstadt (15) described an experiment where they used a dye laser to excite atomic fluorescence of several elements. Tunable dye lasers (16) are nearly ideal sources for AFS (except for their cost). The unique properties of tunable dye lasers include high spectral

irradiance over a narrow spectral bandwidth and the wide wavelength tunability over the ultraviolet-visible range. The high spectral irradiance improves linearity of the analytical calibration curve to 3-5 orders of magnitude and may saturate the absorption transition, thus removing the dependence of the fluorescence signal upon the source stability. The linearity of the analytical calibration curve may be improved in two ways due to the high spectral irradiance of lasers. The most obvious is that the low end of the calibration curve may be extended due to lower detection limits, until optical saturation has been reached. The other way is by eliminating the prefilter effect which will be discussed in more detail in the next chapter. The spectral bandwidth of the laser beam can be made as narrow as 0.0001 nm or less by inserting a series of tuning elements inside the laser cavity. By utilization of nonlinear crystals, Second Harmonic Generation (SHG), of the laser radiation within birefringent crystals, such as KDP and ADP, results in tunability as low as 217 nm.

Laser-excited atomic fluorescence spectrometry (LEAFS) has been shown to be an extremely sensitive method for trace element analysis (17-20). For the remainder of this chapter, the use of LEAFS will be emphasized.

Atom Reservoir

It is generally stated that the atom reservoir is the weakest link of AFS. In this respect, the use of lasers as an excitation source cannot change the situation. The ideal atomizer or atom reservoir for AFS must combine the following characteristics: good atomization/ionization characteristics, low background emission, freedom from quenching species, long residence time, good stability, high reproducibility, and ease of handling. The three most common atomizers for AFS will be discussed briefly with special emphasis on the ICP.

Despite their popularity, chemical flames have serious limitations when applied to the production of atoms or ions. Hydrogen-based flames generally give low background emission and relative freedom from quenching species, but atomization is poor and interferences are severe. The use of these flames has been restricted to situations in which relatively volatile elements are contained in essentially matrix-free solutions. For most practical analyses, hydrogen-based flames are not useful.

Air-acetylene flames (21) are preferred in AFS, but chemical and ionization interferences often occur and for refractory elements, poor detection limits cannot be avoided. The nitrous oxide flames (22) have been used for their superior atomization capabilities due to higher temperatures. However, the background emission of this

type of flame is higher and can severely degrade the signal-to-noise ratio of the measurements.

The advantages of the electrothermal atomizers, e.g., small sample sizes and low absolute detection limits, are well known. Besides the high atom concentration that is produced during the short atomization cycle, electrothermal atomizers offer the advantage of an inert gas atmosphere by controlling the environment within the atomizer cell. Also, the dilution effect of the analyte by the internal gases is much less than that of analyte species in flames. If scattering is eliminated (e.g., using nonresonance fluorescence lines) and the intense background emission from the incandescent graphite is properly screened, then LEAFS with electrothermal atomizer may be the most sensitive of all atomic spectroscopic techniques. Bolshov et al. (23) have demonstrated that LEAFS with an electrothermal atomizer, which consisted of a graphite tube, offered very high sensitivity for all the elements they studied. However, when working with real samples, Dittrich and Stark (24) have shown that the electrothermal atomizer often suffers severe matrix interferences. Furthermore, the atomization of refractory elements may be a problem and memory effects may occur. In order to inhibit reactions between the analyte and the graphite, Goforth and Winefordner (25) have utilized

various coatings such as the ones used for graphite furnace atomic absorption.

The ICP is the best source of multielement excitation in emission spectrometry (26). Because of the high excitation temperature of the ICP, emission spectra are very rich in atomic and ionic lines causing spectral overlap of many lines to occur. In principle, LEAFS in the ICP should be effective in avoiding these spectral interferences.

There are several reasons why ICPs have proven to be very useful as an atomization or ionization cell for fluorescence spectrometry (27-28). Its high temperature and relatively long analyte residence time ensure a high degree of atomization and/or ionization. These factors increase the freedom from physical and chemical interferences and minimize scattering of the excitation radiation. The argon coolant and aerosol carrier gas used in the ICP provide a chemically inert environment which reduce quenching effects caused by molecular species (as compared to flames), thus increasing the fluorescence quantum yields and the fluorescence signal.

The higher excitation temperature in the ICP increases the population of excited lower levels of any atom or ion resulting in a larger number of suitable transitions for excitation. Since the classical scattering problem which occurs at resonance transitions

can be eliminated by choosing nonresonance transitions, it may be possible to choose an excitation wavelength which is different than an intense fluorescence signal. Therefore, low detection limits will be obtained since the monochromator will not allow the laser radiation scatter to reach the detector. The first study using the ICP as an atomization cell for AFS was reported by Montaser and Fassel (29).

The advantages of combining laser excitation and the ICP as an atom or ion reservoir (30-33) are good sensitivity, low detection limits, and high selectivity. As explained earlier, there is virtually no chance of spectral interferences when laser-excited nonresonance fluorescence is observed. Therefore, the wavelength combination yielding the best detection limits can always be used, whereas the wavelength yielding the best detection limit cannot always be used in ICP emission spectrometry (ICP-ES), where spectral interferences often limit the use of the most sensitive lines.

The disadvantages of the laser-ICP fluorescence system include the complexity of the system, high cost of the equipment, need for different dyes for different wavelength regions, and rapid degradation of dyes. The dye laser can only excite one transition of the analyte atom at a time; thus it is basically a single element technique.

CHAPTER II
PRINCIPLES AND NOMENCLATURE

Theoretical Consideration

The dependence of the atomic fluorescence signal upon the excitation source, experimental configuration, quantum efficiency, and concentration of analyte atoms has been treated extensively in the literature (34-43). Only a brief theoretical treatment applicable to laser excitation will be given in this chapter.

The general expression for the fluorescence radiance, B_F, of a two-level system is given by (36)

$$B_F = \left(\frac{\ell}{4\pi}\right) Y_{21} E_\nu(\nu_{12}) \left(\frac{h\nu_{12}}{c}\right) B_{12} \frac{g_1 n_T}{(g_1+g_2)(E_\nu(\nu_{12})/E^*_\nu(\nu_{12}))+g_1} \qquad (1)$$

where

$E_\nu(\nu_{12})$ = spectral radiance of exciting radiation at the absorption line, ν_{12}, $Wm^{-2}Hz^{-1}$

$h\nu_{12}$ = energy of the exciting photon, J

c = speed of light, ms^{-1}

B_{12} = Einstein coefficient of induced absorption, $m^{-3}J^{-1}s$ Hz

Y_{21} = fluorescence power (quantum) efficiency, dimensionless

ℓ = fluorescence path length in the direction of observation, m

4π = number of steradians in a sphere, sr

g_1, g_2 = statistical weights of levels 1 and 2, respectively, dimensionless

n_T = total concentration of analyte atoms in states 1 and 2, m^{-3}.

The modified saturation spectral irradiance, $E^*_\nu(\nu_{12})$, in $J\ s^{-1}m^{-2}Hz^{-1}$ is given by

$$E^*_\nu(\nu_{12}) = \frac{cA_{21}}{Y_{21}B_{21}} = E^s_\nu(\nu_{12})\ (\frac{g_2+g_1}{g_1}) \qquad (2)$$

where $E^s_\nu(\nu_{12})$ is the saturation spectral irradiance. For a low intensity source $E_\nu(\nu_{12}) << E^*_\nu(\nu_{12})$

$$B_F(Lo) = (\frac{\ell}{4\pi})A_{21}h\nu_{12}(\frac{E_\nu(\nu_{12})}{E^*_\nu(\nu_{12})})(\frac{g_2}{g_1})n_T \qquad (3)$$

or substituting for $E^*_\nu(\nu_{12})$ from equation (2)

$$B_F(Lo) = (\frac{\ell}{4\pi})Y_{21}B_{12}(\frac{h\nu_{12}}{c})E_\nu(\nu_{12})n_T \qquad (4)$$

where A_{21} is Einstein coefficient for spontaneous emission, transition s^{-1}.

For a high intensity source $E_\nu(\nu_{12}) >> E^*_\nu(\nu_{12})$

$$B_F(Hi) = (\frac{\ell}{4\pi}) A_{21} h\nu_{12} \{\frac{g_2}{g_1+g_2}\} n_T \qquad (5)$$

However, if a three-level atomic system is involved, as would be for any stepwise fluorescence transition, the general expression for the fluorescence radiance, B_F, is given by

$$B_F = (\frac{\ell}{4\pi}) A_{32} h\nu_{23} n_T \cdot \{\frac{1}{[1+\frac{g_1}{g_3}(1+\frac{E^*_\nu(\nu_{13})}{E_\nu(\nu_{13})})(1+\frac{g_2}{g_1}\exp(-\Delta E_{12}/kT))+(\frac{A_{32}+k_{32}}{k_{21}})]}\} \qquad (6)$$

where level 3 is the upper level reached after excitation and level 2 is the level reached after radiational decay. The term $E^*_\nu(\nu_{13})$ is defined by

$$E^*_\nu(\nu_{13}) = \frac{cA_{31}}{Y_{31}B_{31}} = \frac{g_3 cA_{31}}{g_1 Y_{31} B_{13}} \qquad (7)$$

where B_{31} = Einstein coefficient of induced emission for process $3 \rightarrow 1$, $m^3 J^{-1} s^{-1} Hz$;

B_{13} = Einstein coefficient of induced (radiative) excitation for process, $1 \rightarrow 3$, $m^3 J^{-1} s^{-1} Hz$;

Y_{31} = the fluorescence quantum efficiency for the radiative process, $3 \rightarrow 1$.

Substitution of $E_\nu^*(\nu_{13})$ into equation (7) results in

$$B_F = \left(\frac{\ell}{4\pi}\right) A_{32} h\nu_{23} n_T \cdot \left\{\frac{1}{\left[1 + \frac{g_1}{g_3} + \left(\frac{cA_{31}}{Y_{31} B_{13} E\nu(\nu_{13})}\right)\left(1 + \frac{g_2}{g_1}\exp(-\Delta E_{12}/kT)\right) + \left(\frac{A_{32}+k_{32}}{k_{21}}\right)\right]}\right\} \tag{8}$$

For a low intensity source, $E_\nu(\nu_{13}) << E_\nu^*(\nu_{13})$

$$B_F(Lo) = \left(\frac{\ell}{4\pi}\right) A_{32} h\nu_{23} n_T \left\{\frac{g_3 E_\nu(\nu_{13})}{g_1 E_\nu^*(\nu_{13})\left[1 + \frac{g_2}{g_1}\exp(-\Delta E_{12}/kT)\right]}\right\} \tag{9}$$

Substituting for $E_\nu^*(\nu_{13})$

$$B_F(Lo) = \left(\frac{\ell}{4\pi}\right) A_{32} h\nu_{23} n_T Y_{31} B_{31} \left(\frac{E_\nu(\nu_{13})}{cA_{31}}\right)\left(\frac{1}{1 + \frac{g_2}{g_1}\exp(-\Delta E_{12}/kT)}\right) \tag{10}$$

For a high intensity source, $E_\nu(\nu_{13}) >> E_\nu^*(\nu_{13})$

$$B_F(Hi) = \left(\frac{\ell}{4\pi}\right) A_{32} h\nu_{23} n_T \left\{\frac{1}{1 + \frac{g_1}{g_3} + \frac{g_2}{g_3}\exp(-\Delta E_{12}/kT) + \left(\frac{A_{32}+k_{32}}{k_{21}}\right)}\right\} \tag{11}$$

According to equations (1) and (6), the most important parameters affecting the fluorescence radiance are the intensity of the source radiation, the concentration of the analyte atoms, the Einstein coefficient of induced absorption and the efficiency of conversion of absorbed to emitted radiation. As indicated by equations (4) and (9), the fluorescence radiance is dependent upon the source radiance and the fluorescence quantum efficiency as long as the spectral radiance of exciting radiation of the absorption line is below the saturation value. However, according to equations (5) and (10) the fluorescence radiance becomes independent of these two parameters when saturation of the upper level is reached. The saturation effect of pumped transition has been treated extensively in the literature (44). Due to the complicated nature of a four-level system, it will not be included in this discussion.

At low optical densities or low atomic concentration, the fluorescence radiance is linearly related to the total concentration of atoms in all states. However, at high optical densities or high atomic concentration, the relationship between the fluorescence radiance and the atomic concentration becomes very complex (45,46).

At high concentration, ambiguities can be introduced due to the geometry of illumination and observation. In order to explain the various effects which may affect the

fluorescence signal at high concentration, consider a square cross-section of an atom reservoir with uniform atom number density and uniform temperature distribution and a parallel beam of primary radiation as well as of observed fluorescence radiation. Such a schematic representation of the geometry is shown in Figure 1 where $L+L_{pre}$ is the pathlength transversed by the excitation beam which passes through the absorbing volume and $\ell+\ell_{post}$ is the pathlength transversed by the fluorescence in the direction of the detector. Assuming that the entire atomic population which is being viewed by the detector is illuminated by the excitation beam, then the cross-section monitored will be $(\ell+L)$. However, several effects may take place at high atomic concentrations which may reduce the intensity of the fluorescence signal.

Assuming that the whole cross-section is examined, a process known as self absorption may occur. This process can be described as the reabsorption of the emitted radiation by the same atomic species which are being measured. The result is a decrease in the fluorescence intensity. In addition, a few specific cases may occur as a function of the illumination and detection geometry. A prefilter effect may result because of the absorption of the excitation beam in a region that is not observed by the detector. Referring to Figure 1, the prefilter effect

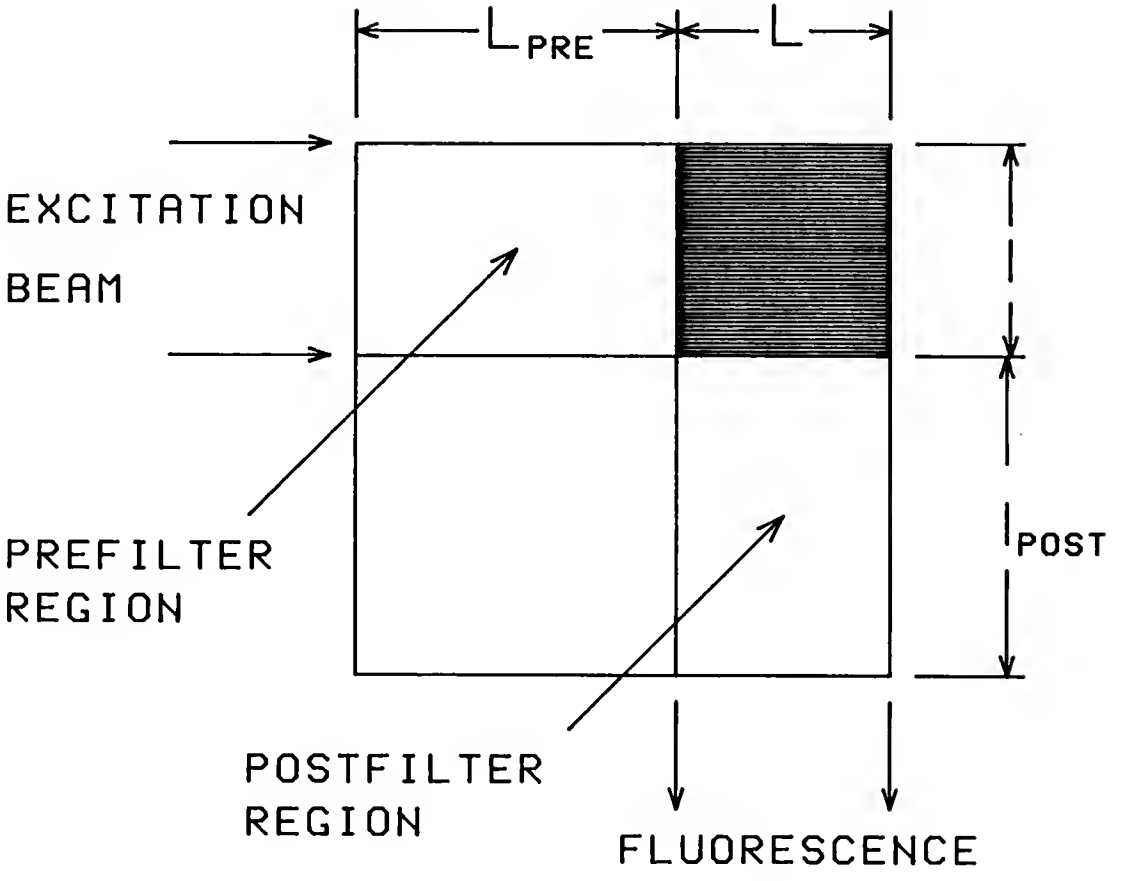

Figure 1. Cross-sectional areas of the atomizer including excitation beam and fluorescence geometry and prefilter and postfilter effects.

depends on the distance L_{pre}; thus if $L_{pre} = 0$ the prefilter effect can be eliminated. A postfilter effect can also occur if there is a region between the illuminated volume and the detector where absorption can reduce the fluorescence intensity. Referring again to Figure 1, the postfilter effect depends on the distance ℓ_{post} and it can also be eliminated if $\ell_{post} = 0$. The self absorption of fluorescent radiation by analyte atom cannot be eliminated by altering the geometry of illumination and detection. All three of these problems only occur at high atomic concentrations; thus they can be avoided by diluting the analyte solution.

Another way to explain the effects which occur at high atomic concentrations is to use curves of growth. A curve of growth in AFS is a logarithmic plot of fluorescence intensity versus atomic concentration or some related function. Zeegers and Winefordner (47) have characterized the shapes of those curves both in theory and experiments. As shown in Figure 2, hypothetical curves of growth for AFS, may take on a negative slope as a consequence of any of the three processes described above. As a consequence of all three processes, the curves of growth may even reach a point where no fluorescence is observed by the detector.

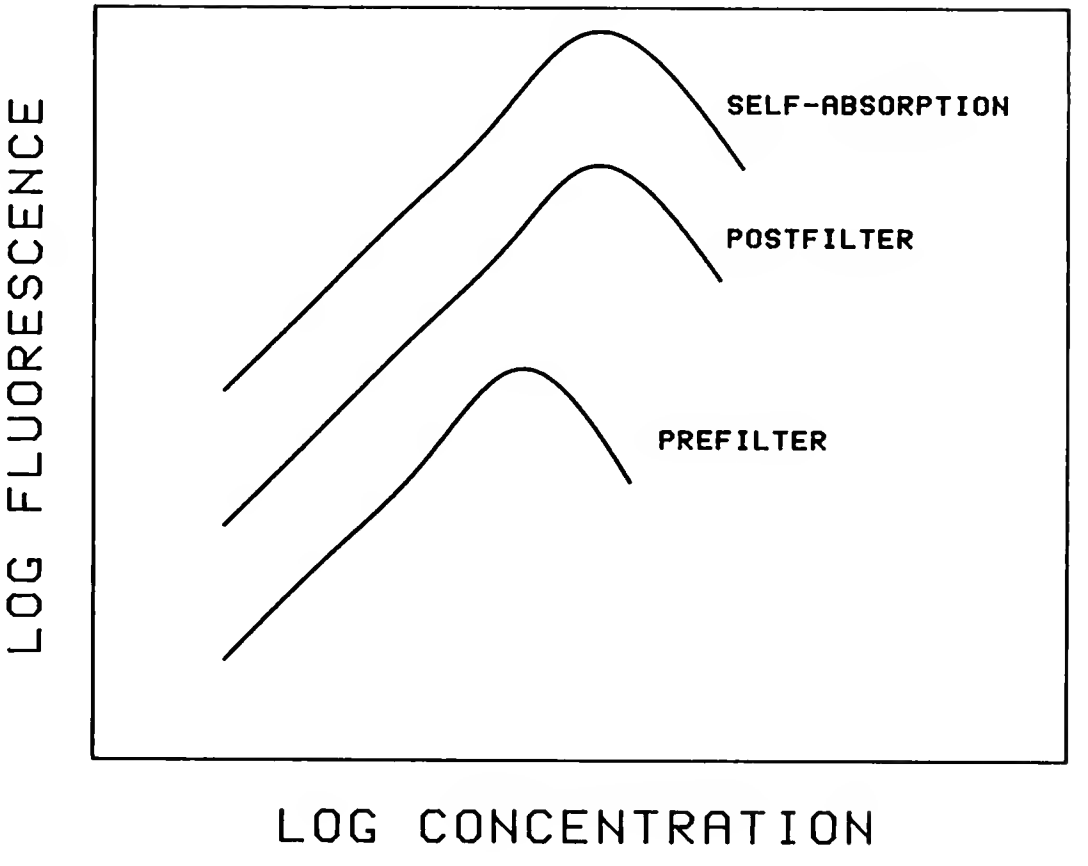

Figure 2. Theoretical fluorescence curves of growth for line source excitation including prefilter, postfilter and self-absorption effects.

Types of Fluorescence Transitions

There has been much confusion among authors concerning the nomenclature of the various types of atomic fluorescence transitions. In order to solve this problem, Omenetto and Winefordner (48) have suggested logical nomenclatures for all of the different types of atomic fluorescence processes. This becomes very important when dealing with dye laser excitation because several different types of atomic fluorescence have been observed. There are basically three types of atomic fluorescence, as shown in Figure 3: resonance fluorescence (RF), in which the same lower and upper level are involved in the excitation and de-excitation processes; direct line fluorescence (DLF), in which the same upper level is involved in the excitation and de-excitation processes (but not the same lower levels); and stepwise line fluorescence (SWF), in which different upper levels are involved in the excitation and de-excitation processes. Another type of atomic fluorescence which involves a multi-photon excitation process will be described in Chapter V.

In addition to these three basic types of atomic fluorescence, a number of variations can occur. The fluorescence process is termed Stokes if the excitation energy is greater than the fluorescence energy and anti-Stokes if the fluorescence energy is greater than the

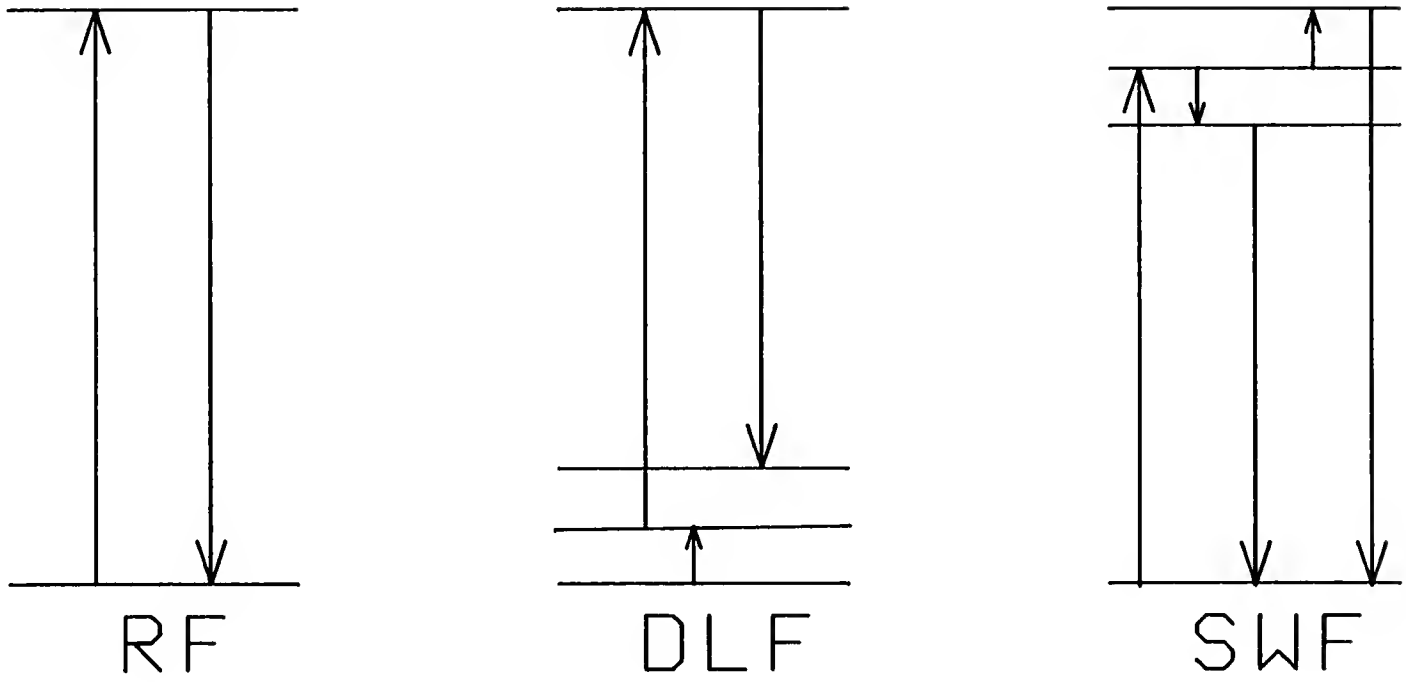

Figure 3. Schematic diagram indicating basic types of atomic or ionic fluorescence transitions.

excitation energy. If both the excitation and fluorescence processes involve only excited states, then it is termed excited-state fluorescence. Finally, if the excitation process involves a collisional excitation following the excitation process, then it is termed thermally assisted. The nomenclature which has been described for atomic fluorescence also applies to ionic fluorescence.

CHAPTER III
ANALYSIS OF RARE EARTHS

Introduction

The rare earths (REs) include those elements of atomic numbers 57 through 71. This group of 15 chemically similar elements are called "REs" because of their relative scarcity at the time this name was proposed and from the fact that their oxides resemble the alkaline-earth oxides. The REs are widely distributed in nature, but concentrated mineral deposits are found only in limited areas. The principal source of the RE material is the mineral monazite which is found in an alluvial sand in Brazil, India and Idaho. This is essentially a complex phosphate, containing as much as 75% REs. The method selected for the extraction of the RE from the ore depends on the nature of the ore and the presence of other elements. They are generally extracted from the minerals by decomposition in sulfuric acid to give the RE metal salt solution. The RE metals and associated salts are now neither rare nor unavailable.

The chemical similarity among each individual RE element depends upon similarities in electronic

configurations in the atoms and derived ions. Because of the essential constancy of the resulting outermost electronic arrangement, beyond lanthanum, it becomes easier for added electrons to enter a more deeply buried arrangement (4f) where space for a total of 14 electrons exists. It is the filling up of this 4f shell which leads to the RE series. This phenomenon is reflected by remarkable similarities in crystal structures, solubilities, and chemical characteristics.

Analytical Measurements

Unfortunately, the REs have been least investigated by spectroscopists. This is mainly because of the difficulty in separating and purifying these elements and especially because of the extreme complexity of some spectra. The great similarity in the chemical properties of the REs has made their separation difficult.

The analytical requirements for the determination of the RE require that the instrument used for analysis must achieve detection limits below 0.1 μg/g. Before the introduction of ICP analysis, almost all published RE determinations were done either by neutron activation (49,50) or isotope dilution mass spectrometry (51). The sensitivities obtained by these two methods are good but they are slow and expensive. Other methods for the quantitative determination of individual REs include

emission, x-ray, arc and spark spectra, and chromatography. The application of ion exchange techniques to RE analysis has proven to be successful for their separation. Accurate RE analysis by x-ray spectroscopy has proven to be difficult because of the comparatively large size of the RE nucleus. Because of the relatively poor sensitivity and also the great number of lines in arc and spark spectrometry, it is difficult to measure individual REs in a mixture. An example of the complexity of their spectra is indicated by the arc emission spectra of cerium. Corliss and Bozman (52) have classified almost 2,000 emission lines for this element.

In 1967, Ovchar and Poluektov (53) studied the atomic emission of the RE in an air-acetylene flame. However, their best detection limits were approximately 200 ppm. Then in 1969, a major advance in the spectrometric analysis of RE resulted from the work of Knisely, Bottler and Fassel (54). They discovered that the fuel-rich nitrous oxide-acetylene flame could produce and excite free atoms of the REs. Their results showed much improvement in detection limits due to the higher temperature of this type of flame. Their best detection limits were 10 ppm. Then in 1972, Crock and Lythe (55) used the method of ICP-ES for the determination of REs. Their best detection limit was down to 0.9 ppm. The high sensitivity as well as rapid and reliable measurement of

REs by ICP-ES (56-58) provides an attractive alternative to the conventional methods used in the past. It was determined that when REs are excited by means of an ICP, a high percentage of ions is achieved because the first ionization potential ranges from 5 to 7 electron volts. Therefore, the intensity of the ionic lines are likely to be much greater than the atomic lines.

In 1980, Houk et al. (59) developed a new technique called ICP-MS. In this approach, the plasma is not used as a source of light but as a source of ions. These ions are almost entirely atomic and are detected with a quadrupole mass analyzer. This technique provides excellent sensitivity, a simple spectra and the possibility of measuring isotopes. Detection limits as low as 0.02 ppb have been achieved for the measurement of REs.

Uses and Applications

One of the oldest applications of REs has been to improve the properties of high temperature alloys. The RE metals have profound influence on the formation, shape and distribution of nonmetallic fractions in iron and steel. For example, in the steel industry, the addition of RE improves the hot workability and increases resistance to corrosion and oxidation (60). The addition of RE metals has also been shown to improve the electrical and thermal conductivities of copper base alloys (61).

Industrial utilization of REs is very important in the glass and ceramic industries (62). They are especially used for polishing glass and for the production of heat resistant optical glass filters. Because of the property of ultraviolet ray absorption possessed by the REs, they have been used in the making of sunglasses and welder goggles.

The determination of rare earths (REs) in silicate rocks is of fundamental importance to modern studies of petrogenesis. Rare earth distributions provide valuable data in crystal and mantle evolutionary processes thus helping our fundamental understanding of the processes by which rocks are formed. The measurement of the concentrations of these elements in various rock types has initiated much research by geochemists in recent years because it can provide them with the origins of these rocks. Finally, applications of the REs in industrial chemistry (63) include catalysts, promoters, phosphorus, activators, and solid state physics and electronics.

CHAPTER IV
ANALYTICAL STUDIES OF LASER-EXCITED IONIC FLUORESCENCE (ONE-STEP)

Introduction

The goal of this study was to investigate the usefulness of a pulsed tunable dye laser for excitation of fluorescence of the RE in the ICP. It was believed that laser-excited ionic fluorescence spectrometry (LEIFS) of RE would overcome the spectral interferences obtained when doing trace elemental analysis by ICP-ES.

Although the emission of the RE in the ICP has been amply described, the ionic fluorescence characteristics of the RE in the ICP have never been reported. This chapter will report on the ionic fluorescence of the RE elements by pulsed dye laser excitation in the ICP.

Because of the striking simplicity of the RE fluorescence spectra, which results with narrow bandwidth dye laser excitation and gated detection, it is possible to reduce greatly or even eliminate spectral interferences in a mixture of all the REs. Furthermore, detection limits as low as 25 ppbs were achieved.

Selection of Transitions for Laser-Excited Ionic Fluorescence Measurements in the ICP

From equation (7) it is possible to give an expression which expresses the effect of each term upon the selection of an optimum excitation and fluorescence transition. Since most excitation and fluorescence transitions which were investigated involved a three-level system, only this example will be examined. If all terms not related to either the excitation or fluorescence processes are included in a constant K' and it is assumed that $A_{31} << (k_{31}+k_{32})$ and $\frac{g_2}{g_1} \exp(-\frac{\Delta E_{12}}{kT})$ is negligible, then equation (6) is reduced to

$$B_F = K'[(g_3A_{32})\nu_{32}]_{em}[(g_3A_{31}) \frac{E_\nu(\nu_{13})}{\nu_{31}^3(k_{31}+k_{32})}]_{exc} \quad (12)$$

According to equation (12), it is desirable to select an excitation wavelength which possesses a high transition probability value, g_3A_{31}. It is also desirable to select a fluorescence wavelength which possesses a high transition probability value, g_3A_{32}. Therefore, the selection of excitation and fluorescence transitions for LEIF measurements in the ICP can be made on the basis of their gA values. Of course it is also desirable to select an excitation transition which originates from the ground ionic state or a level near the ground ionic state.

The next step is to find a probable fluorescence transition which originates from the upper level of the excitation transition. If one cannot find such a transition, then a fluorescence transition from a level which is close to the upper level of the excitation transition can be used. Once the excitation and fluorescence transitions have been chosen, the monochromator is set to the probable fluorescence wavelength and the laser is scanned slowly in the region where excitation is most likely to occur. Once a fluorescence signal has been observed, then the laser is tuned to obtain a maximum signal. At this point, the excitation wavelength has been achieved and the emission monochromator is scanned from 250 to 700 nm to determine the most intense fluorescence wavelengths.

Corliss and Bozman (52) have determined experimental transition probabilities and energy levels for several spectral lines of the REs. These tabulated values were very useful in selecting the wavelengths of excitation in this thesis work. However, it is not possible to predict exactly the optimum combination of wavelengths for excitation and fluorescence. The best combinations of wavelengths must be determined experimentally.

Experimental

Instrumentation

A block diagram of the laser-excited ICP system is shown in Figure 4. The dye pumping source in the set-up is a rare gas halide excimer laser (Lumonics, Ontario, Canada, Model TE-851-S), operated with XeCl at 308 nm. A maximum energy output of 60 mJ per pulse was obtained at a repetition rate of 25 Hz. The laser beam energy was monitored before each measurement with a power meter (Scientech Inc., Boulder, Colorado, Model 380105).

A frequency doubled (KDP) tunable dye laser (Lumonics, Ontario, Canada, Model EDP-330) was used to cover the desired spectral range. One dye laser medium was made by dissolving 0.199 g of DPS dye (Exciton Chemical Co., Inc., Dayton, Ohio) in 1.000 L of dioxane. A fundamental output of 200 to 250 kW peak power was obtained between 400 and 412 nm. Another dye laser medium was made by dissolving 0.184 g of rhodamine 610 dye (Exciton Chemical Co., Inc., Dayton, Ohio) in 1.000 L of deionized water. The third dye laser medium was made by dissolving 0.119 g of PBD dye (Exciton Chemical Co., Inc., Dayton, Ohio) in 1.000 L of a 1/1 mixture of toluene and ethanol. A frequency doubled output of 10 to 14 kW peak power was obtained between 298-306 nm. The pulse width and spectral bandwidth of the dye laser output was 8 ns and 0.004 nm, respectively. Wavelength selection was

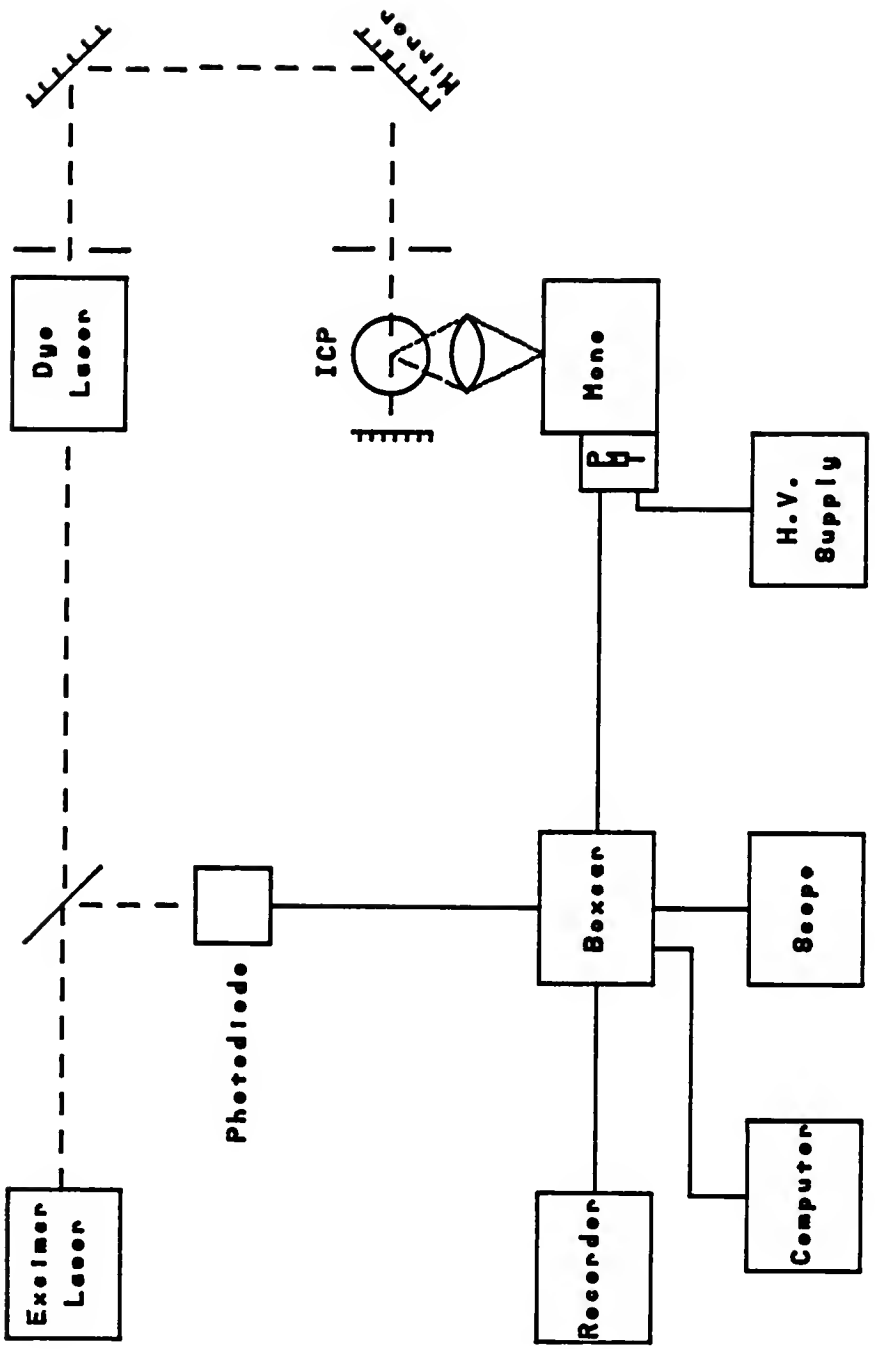

Figure 4. Block diagram of experimental system for laser-excited ionic fluorescence of the rare earth elements in the inductively coupled plasma (one-step excitation).

carried out with an automatic scanning unit (Compuscan, Lumonics, Model EDP-60).

The ICP was a standard 27 MHz commercial model (Plasma Therm Inc., Kresson, New Jersey, Model HFP-1500). Typical operating parameters were incident power of 0.6 to 1 kW; plasma support argon gas flow rate of 12 to 15 L min^{-1}; auxiliary argon gas flow rate of 0.5 to 1.1 L min^{-1}; and viewing height above the load coil of approximately 15 mm. The reflected power was minimized by the automatic matching network in the power supply. The sample was introduced into the plasma with a concentric nebulizer. A nebulizing gas pressure of 32 psig produced a solution uptake of 1.1 mL/min. The ICP torch was mounted on an adjustable mount in order to facilitate optimization of viewing heights without changing the alignment of the laser and detection system.

As shown in Figure 2, the laser beam was directed into the ICP by means of two plane mirrors. A third plane mirror allowed a second pass of the laser radiation when frequency doubling was used. Two small apertures (2 mm) were placed in the excitation direction. One was placed 5 cm away from the output of the dye laser and the other one 40 cm away from the plasma. Because of the slight divergence of the laser beam, the laser beam diameter in the ICP was measured to be approximately 3 mm.

The resulting fluorescence from the laser irradiated volume was focused as a 1:1 image on the entrance slit of the 0.35 m monochromator (Heath, Benton, Harbor, Michigan model). A 3 mm slit height and a 150 µm slit width was used. Neutral density filters were used to increase the linear dynamic range. A photomultiplier tube (Hamamatsu, Inc., Middlesex, New Jersey, Model R928) operated at -1000 Volts D.C. was used to measure the intensity of the fluorescent radiation. The photomultiplier tube base was modified for fast response (17).

Since the laser output was made up of 8 ns pulses at a rate of 25 Hz, the output of the PMT was fed into a gated integrator and boxcar averager (Stanford Research System, Palo Alto, California, Model SR 250) which was triggered by a photodiode positioned to collect a portion of the laser radiation. The gate width was set at 200 ns and the gate delay at 34 ns. The output signals of the gated integrator and boxcar averager were displayed on a strip chart recorder and measured with a personal computer.

Chemicals

All RE standard stock solutions were prepared by dissolving a sufficient amount of the rare earth oxide (Spex Industries, Inc.) in a minimal volume (3 to 5 mL) of hot hydrochloric acid and then diluting in enough

deionized water to make 100 mL of 1000 μg mL^{-1} solution (64). The only exception was for ceric ammonium nitrate which was dissolved in water. Working standards were made by serial dilutions from 1000 ppm stock solutions. All solutions were stored in polyethylene bottles.

Results and Discussion

Analytical calibration curves were constructed for the laser-excited ionic fluorescence (LEIF) of all the REs except for promethium, because this chemical was not available, and holmium, because no ionic fluorescence was detected for this element. Analytical curves are given for all the REs in Figures 5-17; detection limit of REs by LEIF are reported in Table 1. All measurements were obtained at nonresonance fluorescence lines. The use of nonresonance instead of resonance fluorescence resulted in a decrease in the detection limit by a factor of up to 10X due primarily to the minimization of measuring scattered radiation from the source. From the results shown in Table 1, it is observed that for all REs, the ionic fluorescence LODs are approximately 10X inferior to the best one reported by ICP-ES (59) with a pneumatic nebulizer.

In order to reach the wavelengths below 350 nm, it was necessary to frequency double the output of the dye

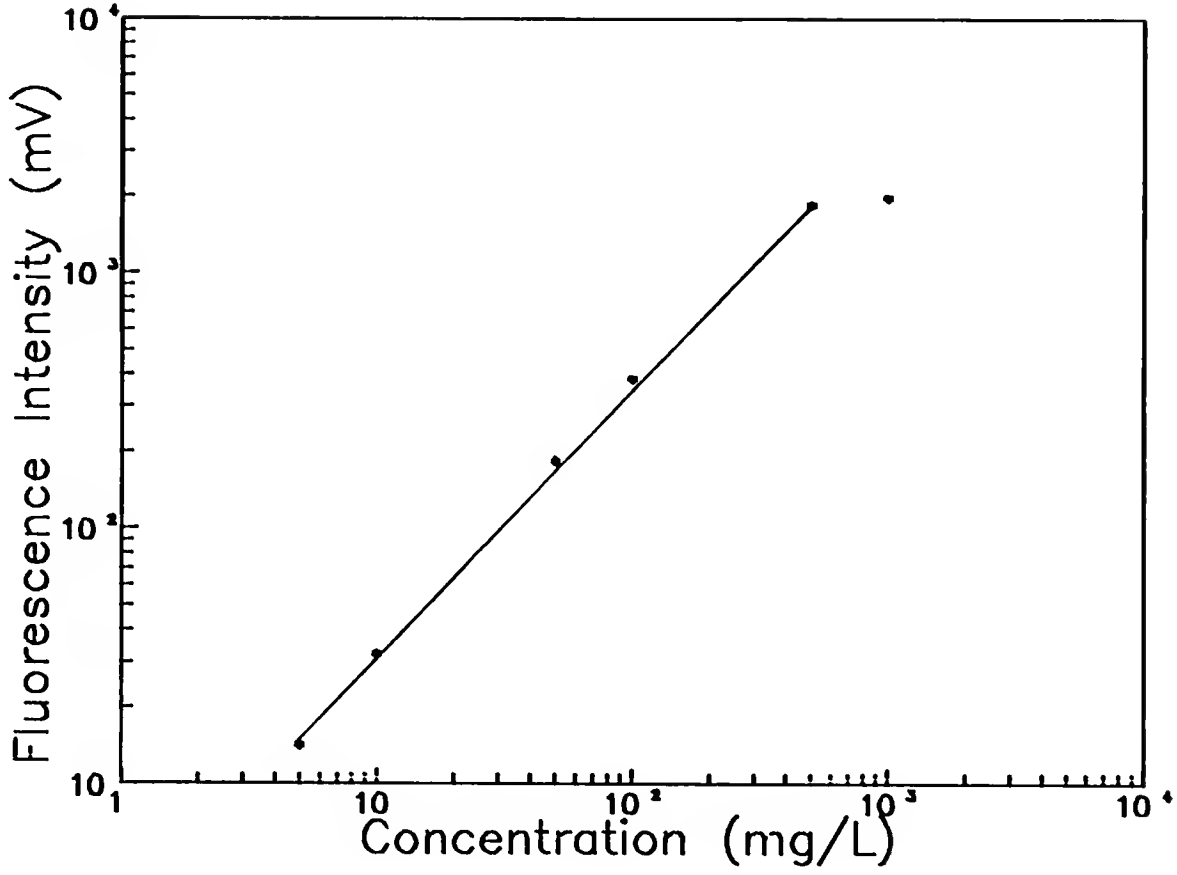

Figure 5. Analytical calibration curve for ionic fluorescence of lanthanum (excitation at 407.735 nm and detection at 399.975 nm).

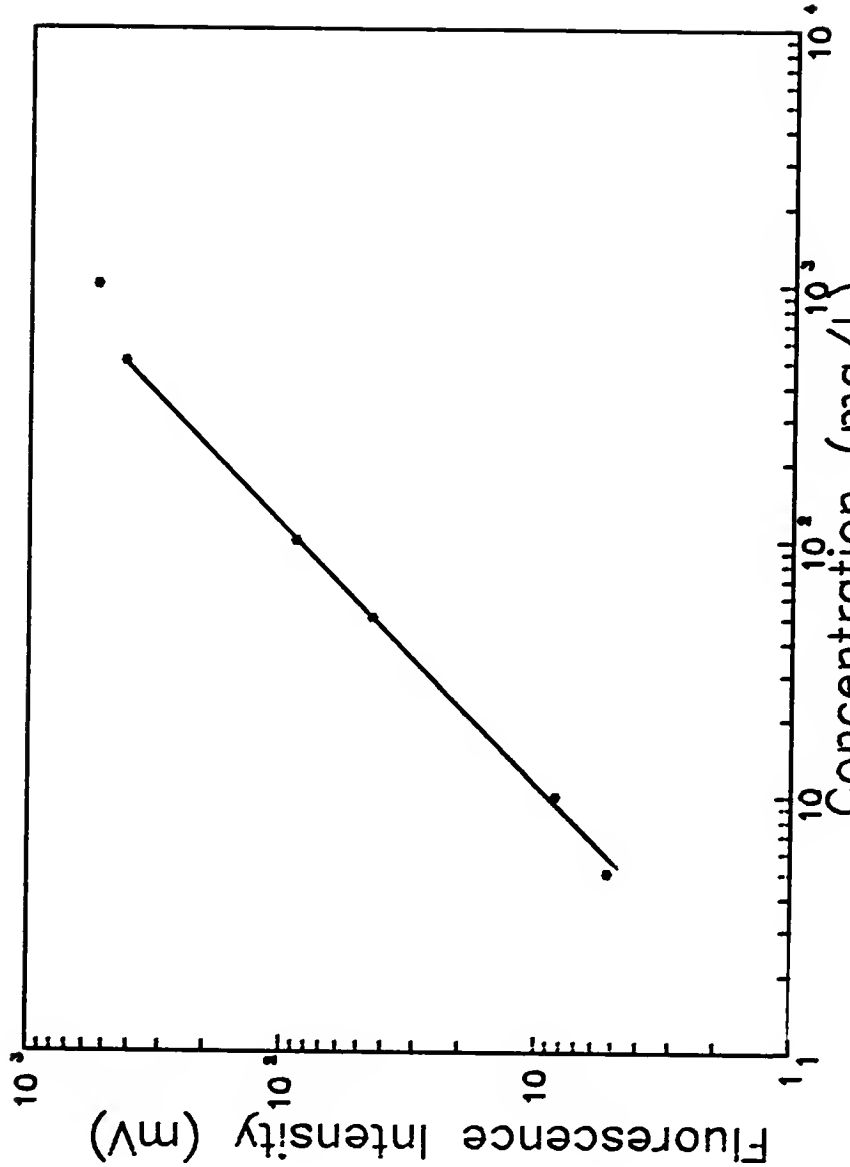

Figure 6. Analytical calibration curve for ionic fluorescence of cerium (excitation at 407.585 nm and detection at 401.239 nm).

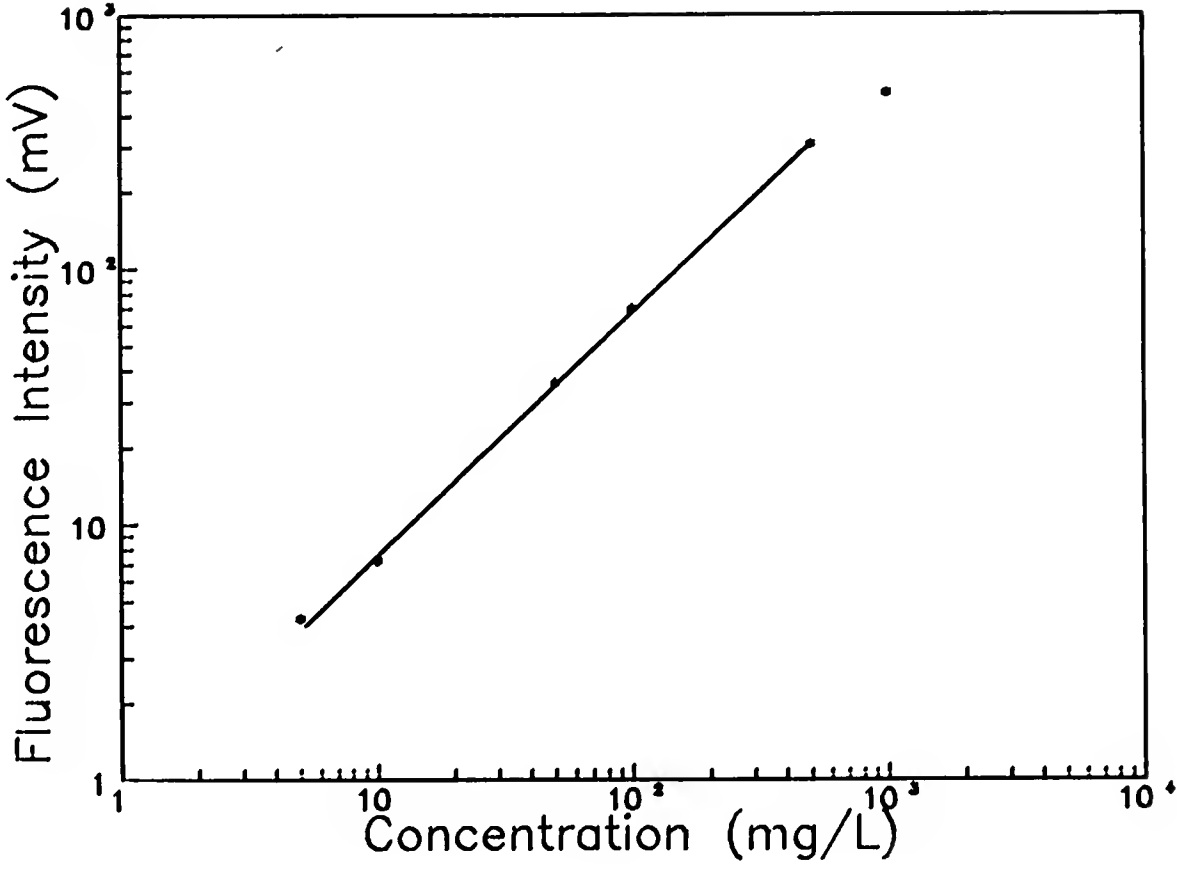

Figure 7. Analytical calibration curve for ionic fluorescence of praseodymium (excitation at 406.282 nm and detection at 406.282 nm).

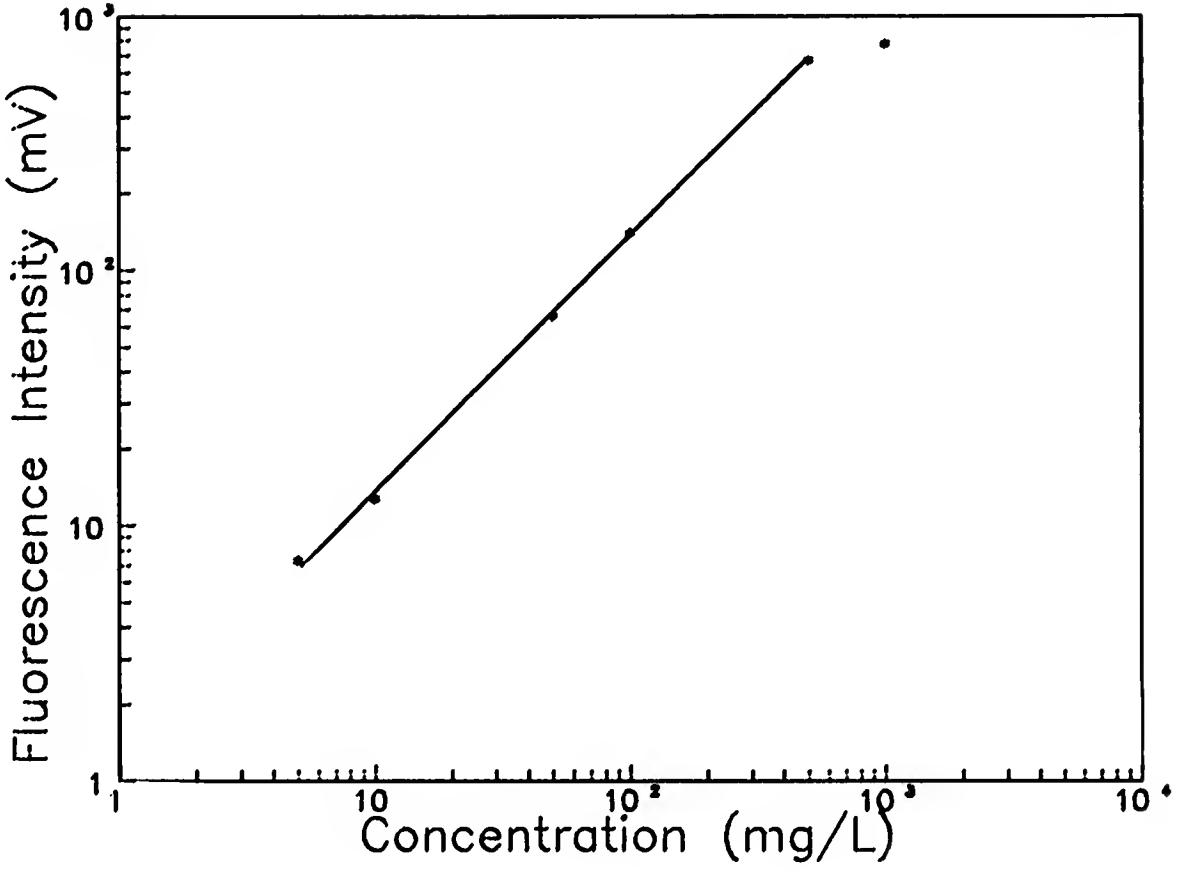

Figure 8. Analytical calibration curve for ionic fluorescence of neodymium (excitation at 406.109 nm and detection at 428.452 nm).

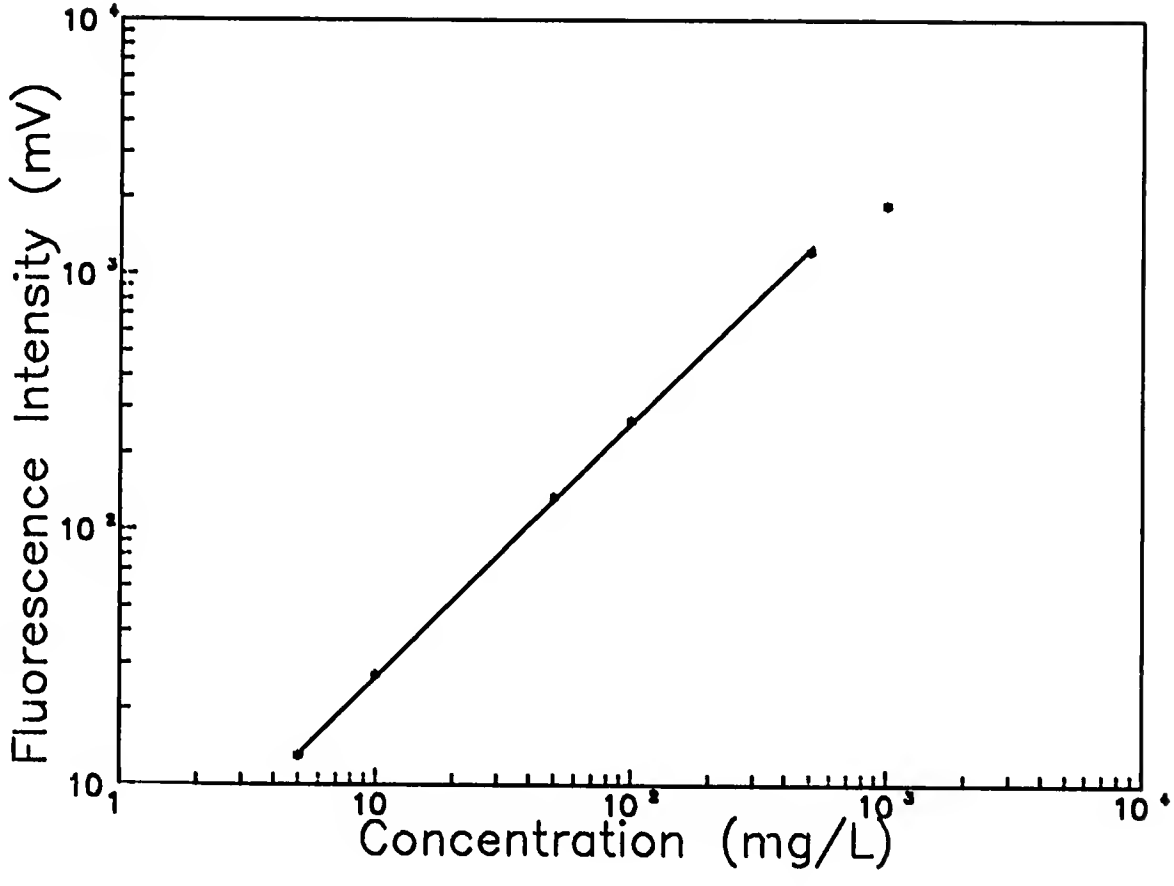

Figure 9. Analytical calibration curve for ionic fluorescence of europium (excitation at 299.133 nm and detection at 290.668 nm).

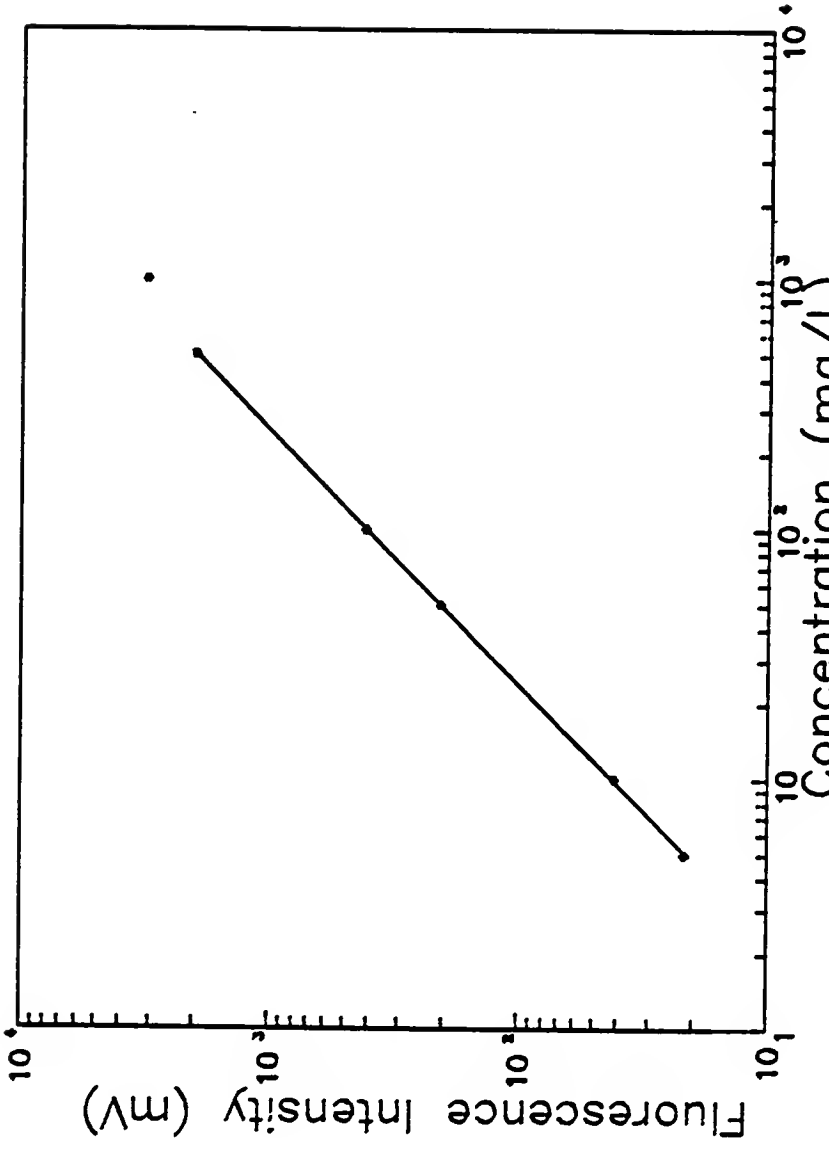

Figure 10. Analytical calibration curve for ionic fluorescence of gadolinium (excitation at 407.844 nm and detection at 354.580 nm).

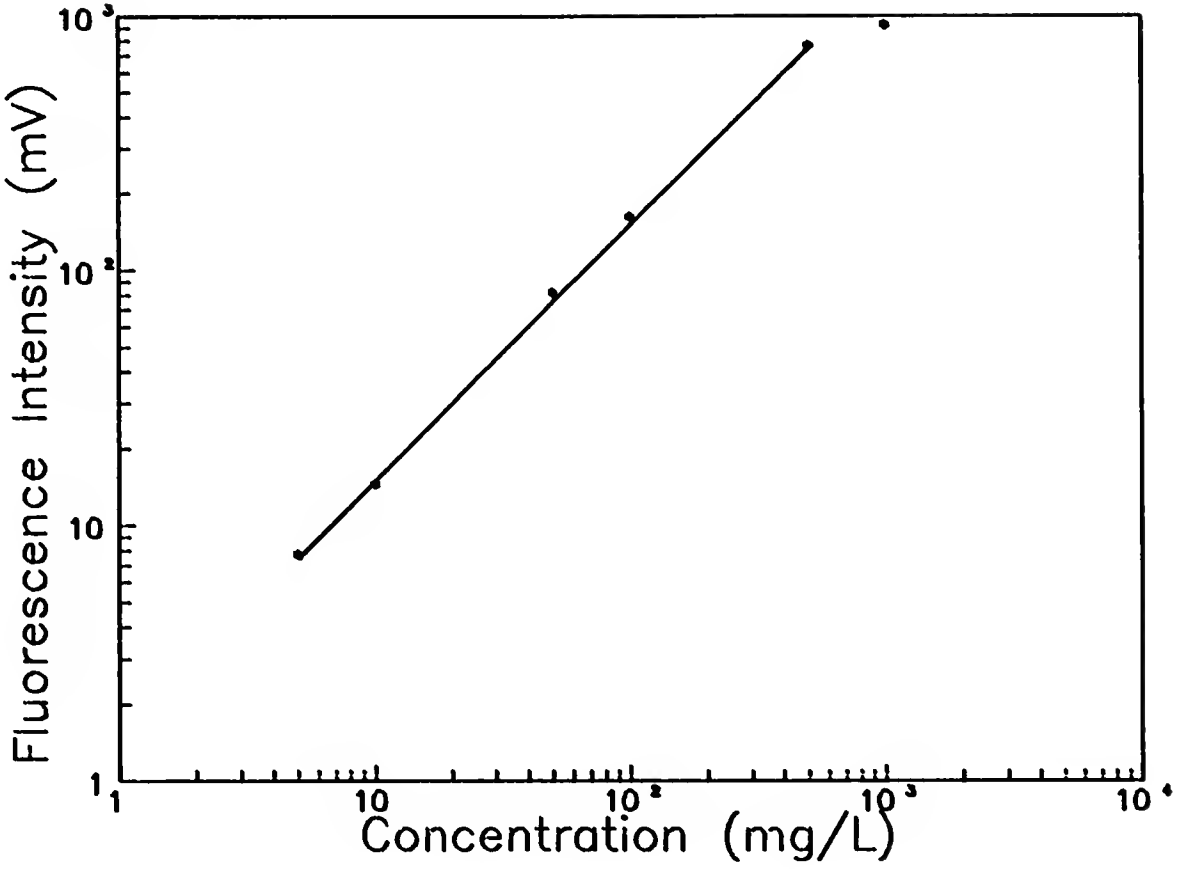

Figure 11. Analytical calibration curve for ionic fluorescence of dysprosium (excitation at 407.798 nm and detection at 394.470 nm).

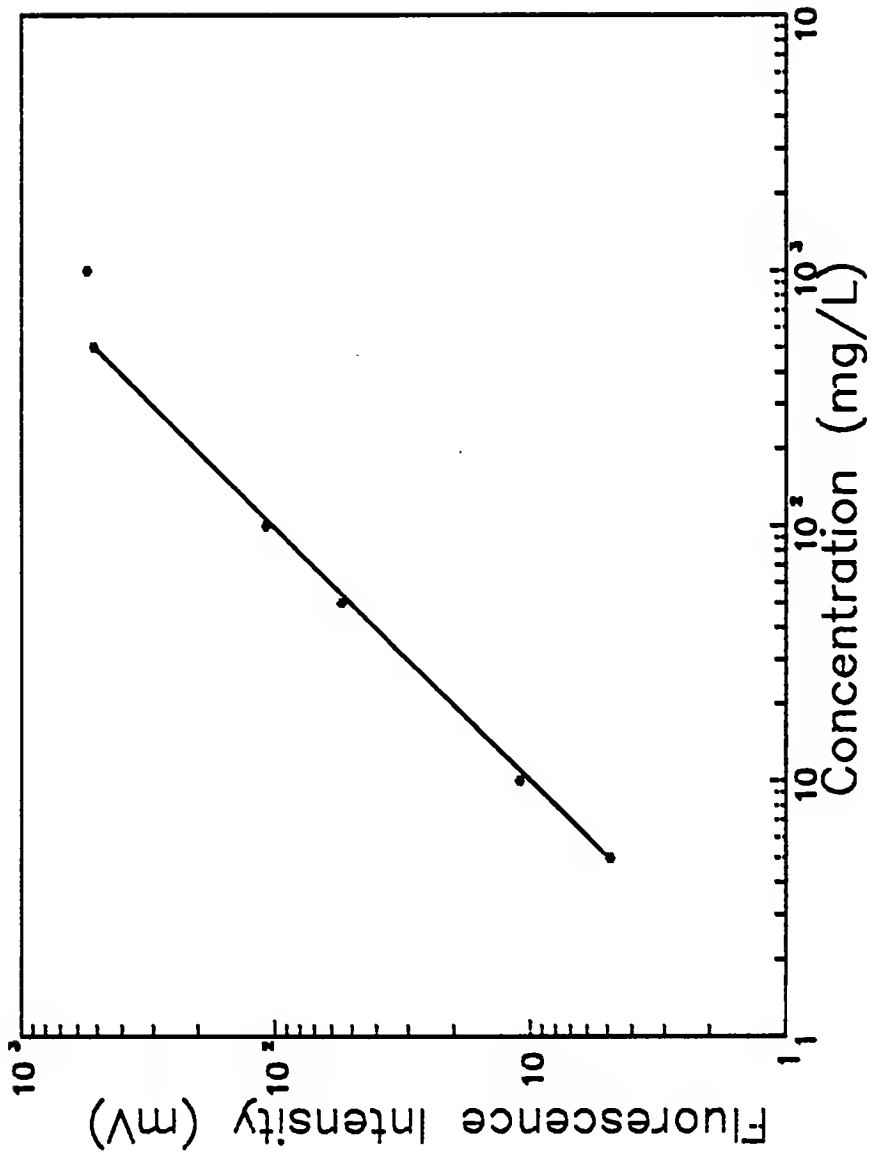

Figure 12. Analytical calibration curve for ionic fluorescence of erbium (excitation at 410.400 nm and detection at 344.115 nm).

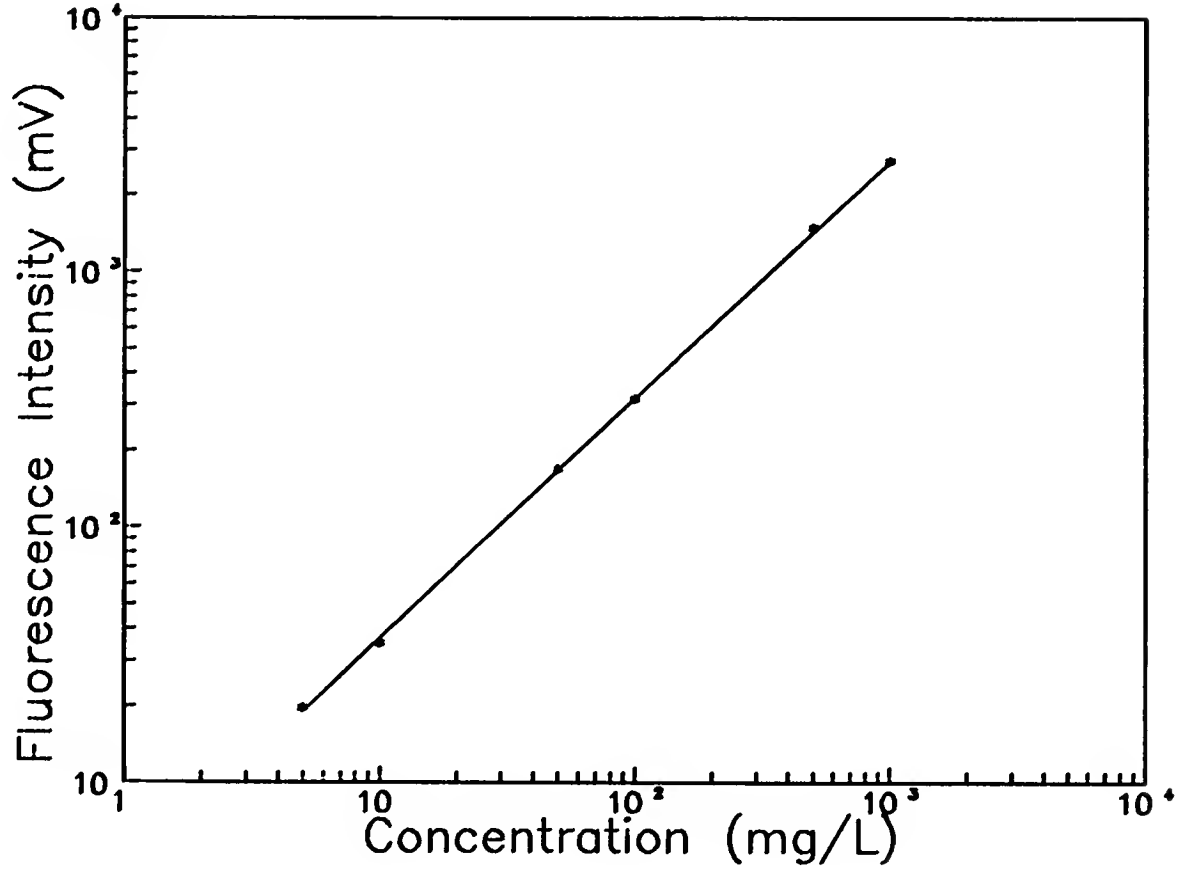

Figure 13. Analytical calibration curve for ionic fluorescence of thulium (excitation at 301.530 nm and detection at 313.136 nm).

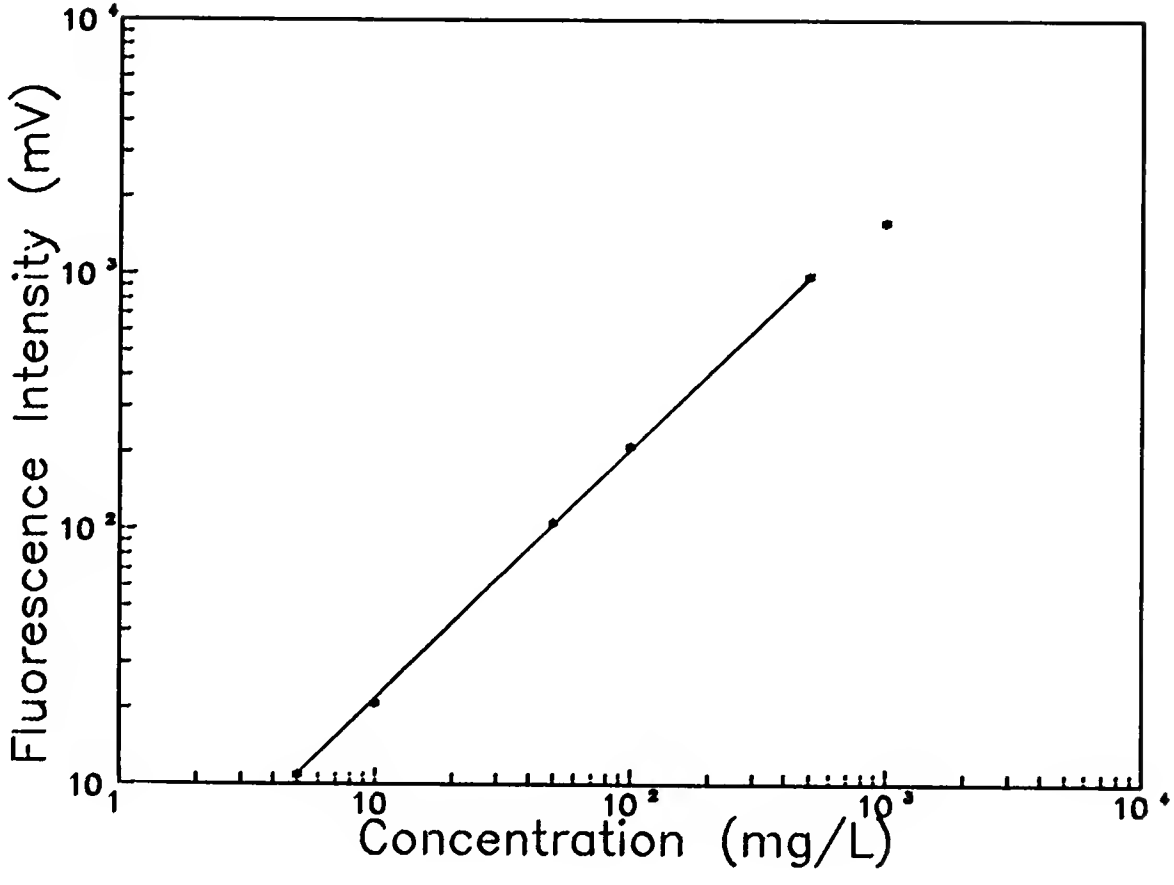

Figure 14. Analytical calibration curve for ionic fluorescence of ytterbium (excitation at 303.111 nm and detection at 297.056 nm).

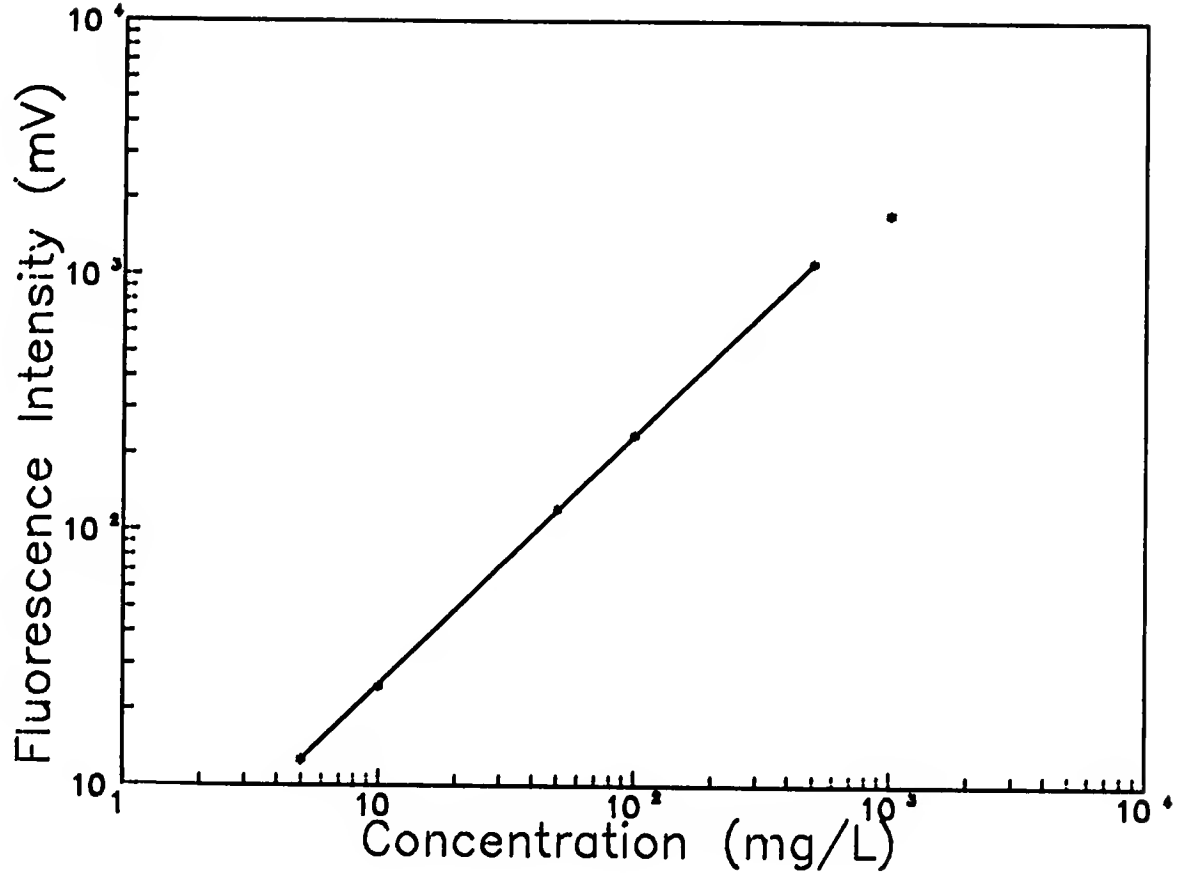

Figure 15. Analytical calibration curve for ionic fluorescence of lutetium (excitation at 302.054 nm and detection at 296.332 nm).

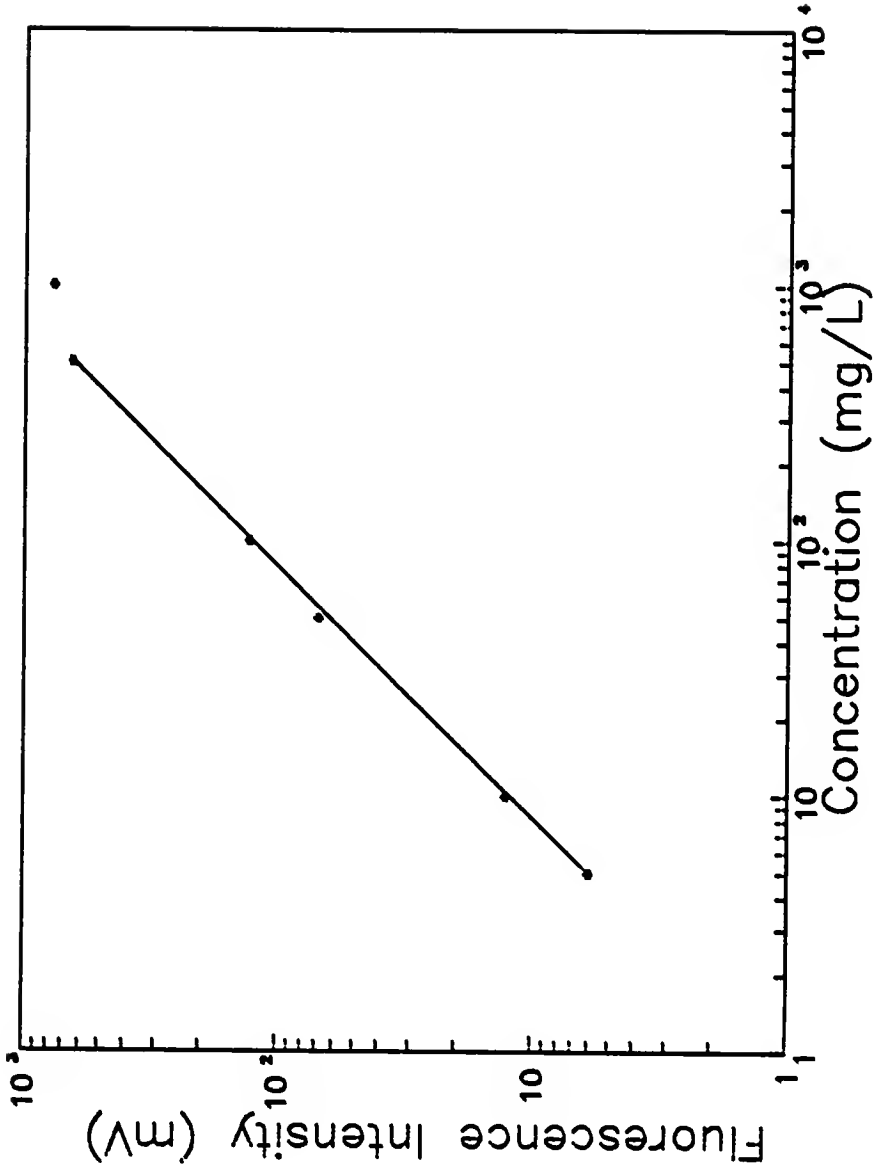

Figure 16. Analytical calibration curve for ionic fluorescence of samarium (excitation at 366.136 nm and detection at 373.126 nm).

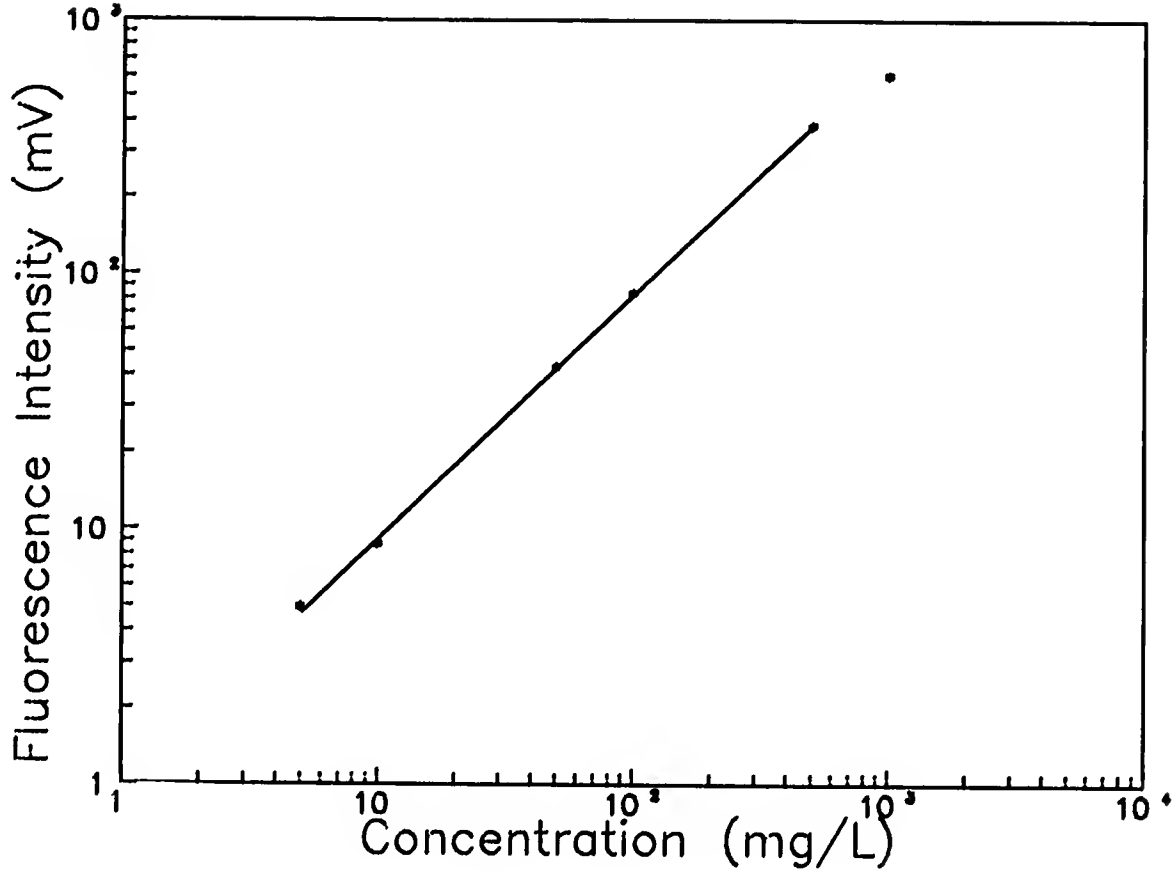

Figure 17. Analytical calibration curve for ionic fluorescence of terbium (excitation at 403.306 nm and detection at 400.557 nm).

Table 1. Fluorescence transitions and detection limits for the rare earth elements in the inductively coupled plasma (one-step excitation).

Rare Earth Element	Excitation Wavelength (Transition, cm^{-1})[a] ℓ --> u	Fluorescence Wavelength (nm) (Transition, cm^{-1})[a] u --> ℓ	Fluorescence Process[b]	Detection Limit[e] (ng/ml)	Detection Limit by ICP-ES (ng/ml)[c]
La	407.735 (1895 - 26414)	399.975 (1394 - 26414)	S-DLF	160.	10.
Dy	407.798 (828 - 25343)	394.470 0 - 25343)	AS-DLF	390.	10.
Gd	407.844 (4841 - 29353)	354.580 (1159 - 29353)	AS-DLF	75.	14.
Ce	407.585 (4911 - 29439)	401.239 (4523 - 29439)	AS-DLF	360.	48.
Er	410.400 (5133 - 29492)	344.115 (440 - 29492)	AS-DLF	290.	10.
Nd	406.109 (3802 - 28419)	428.452 (5086 - 28419)	S-DLF	450.	50.
Pr	406.282 (3403 - 28010)	406.282 (3403 - 28010)	RF	290.	37.
Tb[d]	403.306 (?)	400.557 (?)	?	630.	23.
Lu	302.054 (12435 - 45532)	296.332 (11796 - 45532)	AS-DLF	85.	1.0

Table 1--continued.

Rare Earth Element	Excitation Wavelength (Transition, cm^{-1})[a] ℓ --> u	Fluorescence Wavelength (nm) (Transition, cm^{-1})[a] u --> ℓ	Fluorescence Process[b]	Detection Limit[e] (ng/ml)	Detection Limit by ICP-ES (ng/ml)[c]
Tm	301.530 (237 - 33392)	313.136 (0 - 31927)	S-SWF	140.	5.2
Yb	303.111 (0 - 32982)	297.056 (0 - 33654)	AS-SWF	25.	1.8
Eu	299.133 (0 - 33420)	290.668 (0 - 34394)	AS-DLF	120.	2.7
Sm	366.136 (327 - 27631)	373.126 (838 - 27631)	S-DLF	460.	43

[a] Energy levels in cm^{-1}; ℓ = lower level; u = upper level.

[b] AS-SWF = Stokes-Stepwise Fluorescence; AS-SWF = Antistokes-Stepwise Fluorescence; S-DLF = Stokes-Direct Line Fluorescence; AS-DLF = Antistokes-Direct Line Fluorescence; and RF = Resonance Fluorescence.

[c] Detection limits from reference 58.

[d] Energy levels were not identified for Tb.

[e] Detection limits have been normalized to a signal-to-RMS noise ratio of 3.

laser resulting in considerably less power for the excitation. Whenever a good excitation transition was available in the region between 400 and 600 nm, it was used since it was possible to excite with the more powerful dye laser fundamental.

The detection limit was defined as being 3 times the standard deviation of the blank solution (water) divided by the sensitivity (the slope of the analytical calibration curve). The standard deviation was determined by collecting 1000 data points at 25 Hz with a personal computer. The high spectral selectivity is evident since the blank signal was the same whether water or a 100 $\mu g\ mL^{-1}$, solution of a mixture of all other REs were aspirated into the plasma.

In all measurements, no spectral interference occurred when 100 $\mu g\ mL^{-1}$ of all the REs were measured. In conventional ICP-ES, spectral interferences in mixtures of REs are serious problems, which necessitated some form of separation prior to the measurements. The unique spectral selectivity associated with laser excited fluorescence is due to the rather narrow spectral bandwidth of the laser, the number densities of the lower levels of the RE species, and the quantum efficiencies of the respective fluorescence transitions.

The analytically useful range or linear dynamic range (LDR) is taken from the detection limit to the upper

concentration where the signal deviates by no more than 5% from linearity. The LDR covers approximately 3 to 4 orders of magnitude. The strong curvature at approximately 1000 ppm for all REs, as shown in Figure 5-17, is probably a result of the combined effects of primary source absorption, self-absorption of fluorescence and reabsorption of fluorescence radiation (postfilter effect).

The pertinent ionic fluorescence transitions for each RE as well as their relative intensities are shown in simplified ionic energy level diagram in Figures 18-29. The transitions shown were selected from NBS Monograph 53 (52). An ionic energy level diagram of terbium is not included because we were not able to identify the energy levels of the transitions corresponding to the fluorescence lines observed. The transitions reported do not represent the complete fluorescence spectrum within the wavelength range studied for each RE, because weaker lines could be observed at higher instrumental gain settings. Although many other ionic fluorescence spectra were observed at different excitation wavelengths, only one ionic energy level diagram per element is given. The use of transitions not involving the ground ionic state was not a problem since the lower ionic energy levels appeared to be highly populated. Excited lower levels may

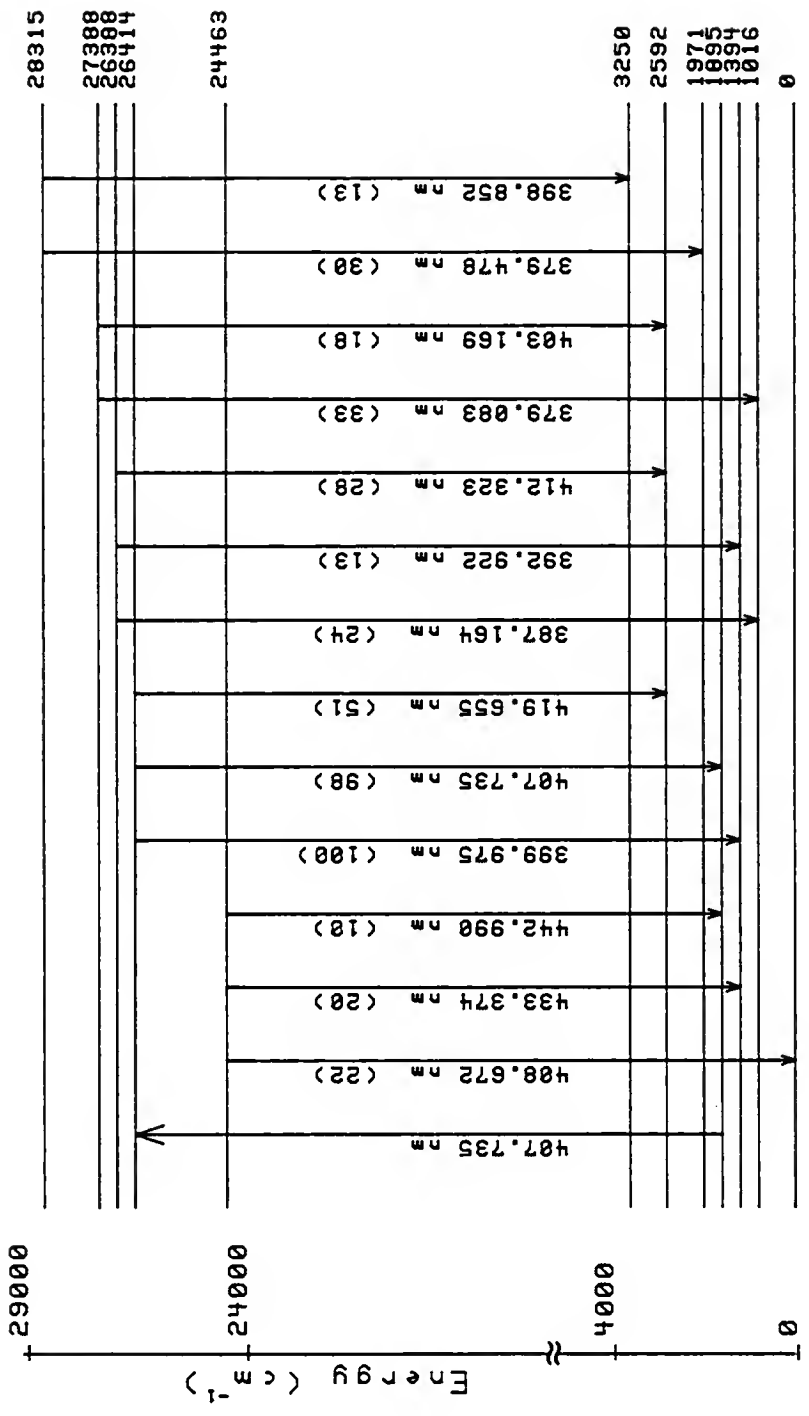

Figure 18. Partial energy level diagram of lanthanum ion (one-step excitation). Wavelengths are also indicated in nm and relative intensities in parentheses.

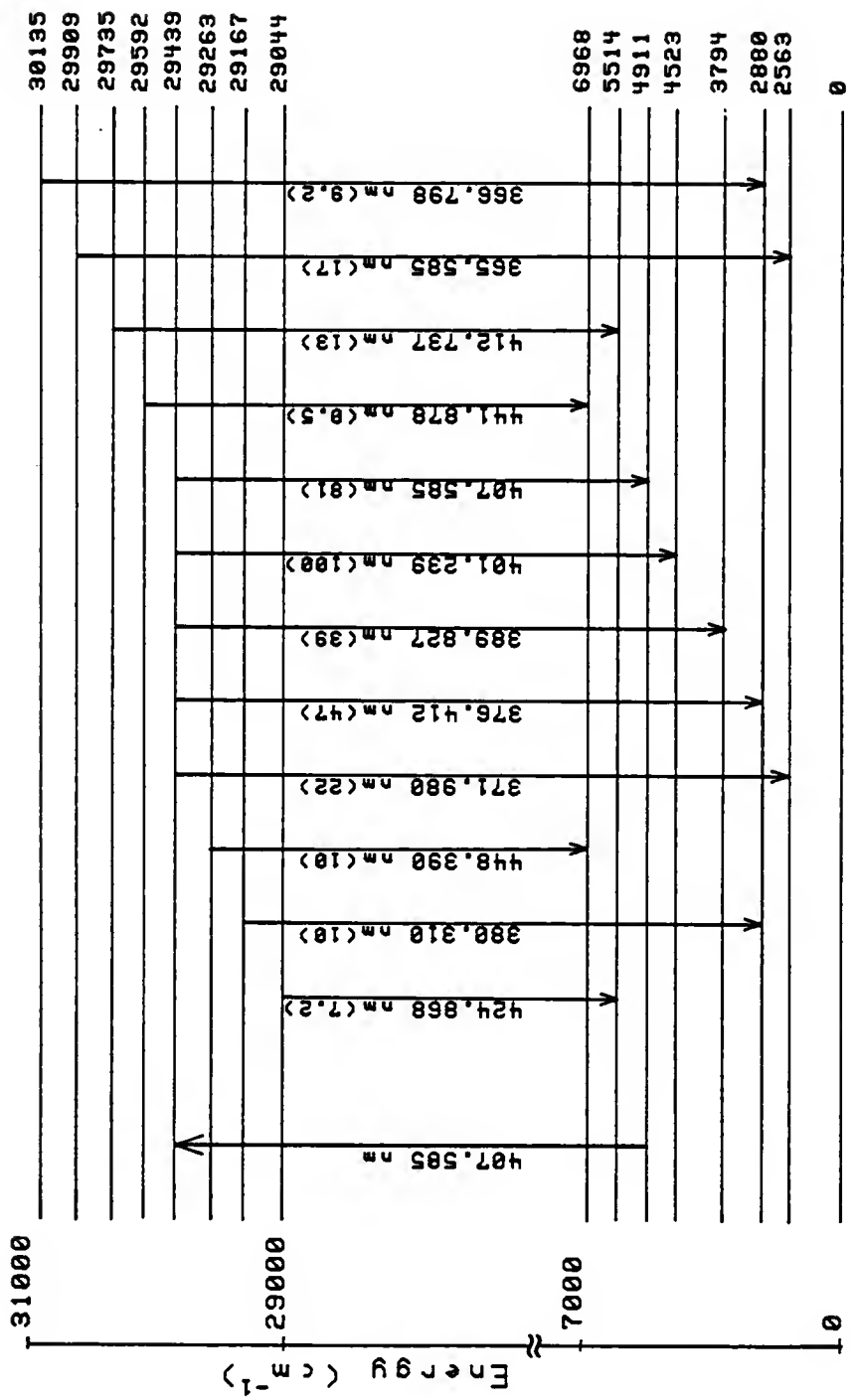

Figure 19. Partial energy level diagram of cerium ion (one-step excitation). Wavelengths are also indicated in nm and relative intensities in parentheses.

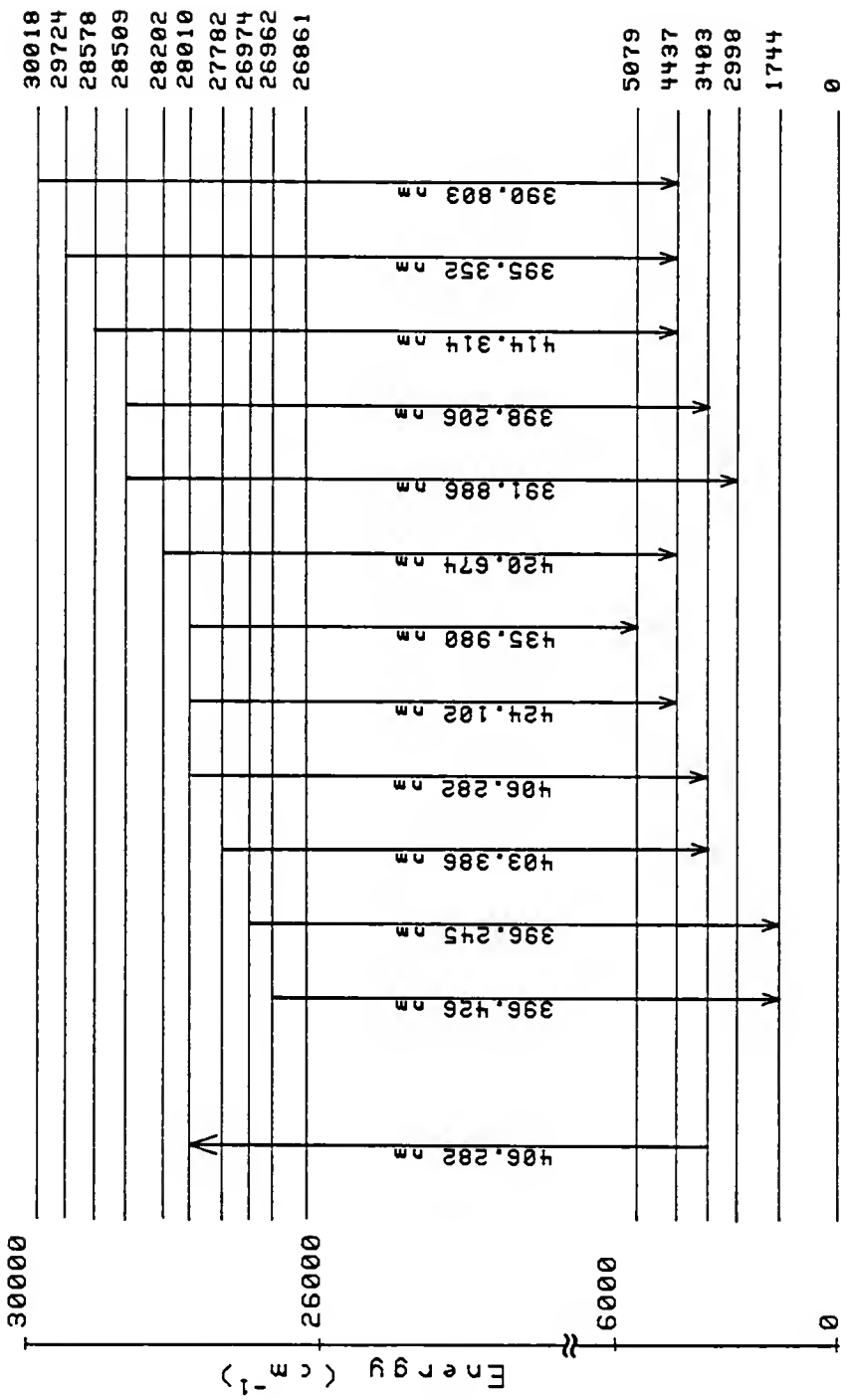

Figure 20. Partial energy level diagram of praseodymium ion (one-step excitation). Wavelengths are also indicated in nm and relative intensities in parentheses.

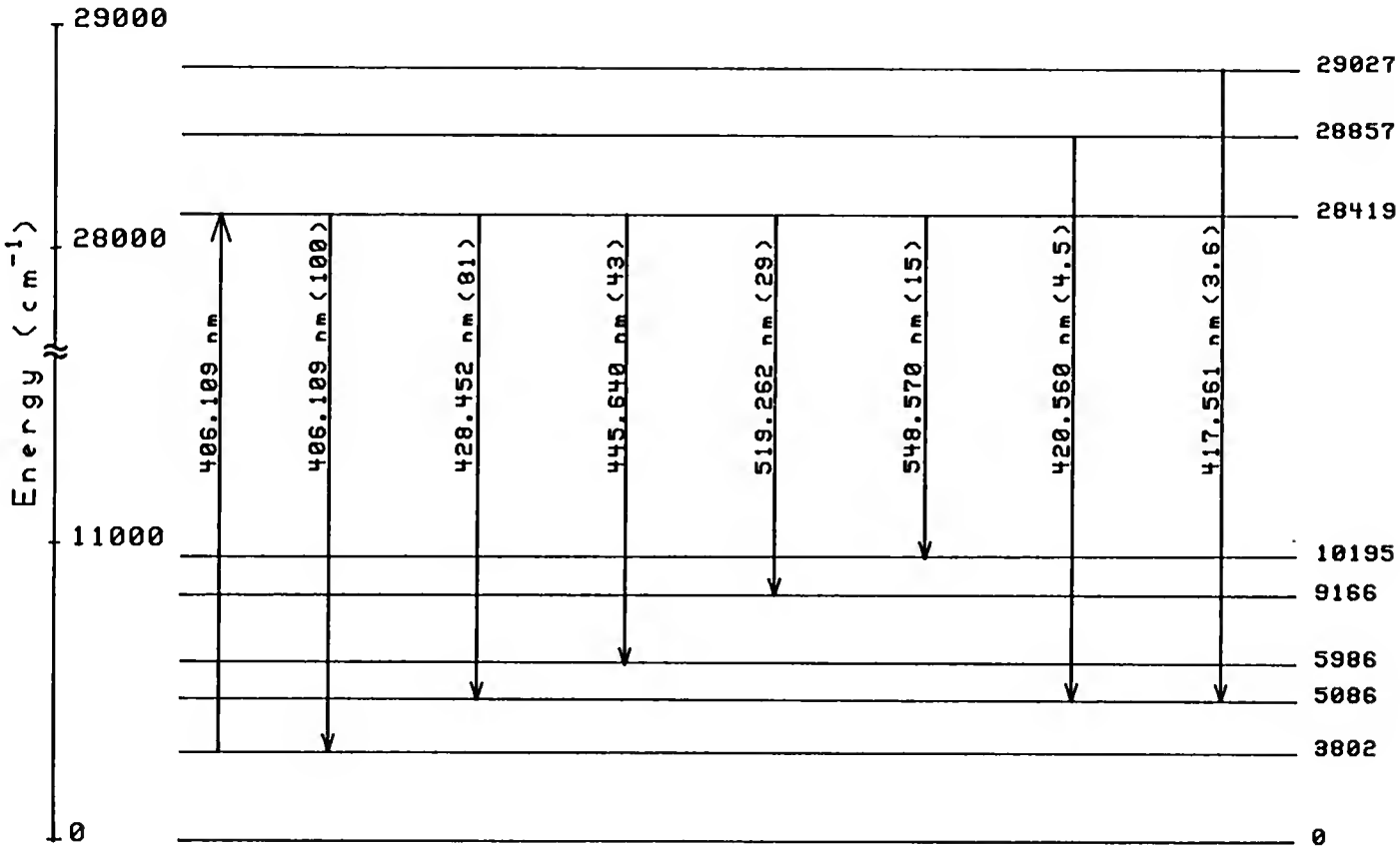

Figure 21. Partial energy level diagram of neodymium ion (one-step excitation). Wavelengths are also indicated in nm and relative intensities in parentheses.

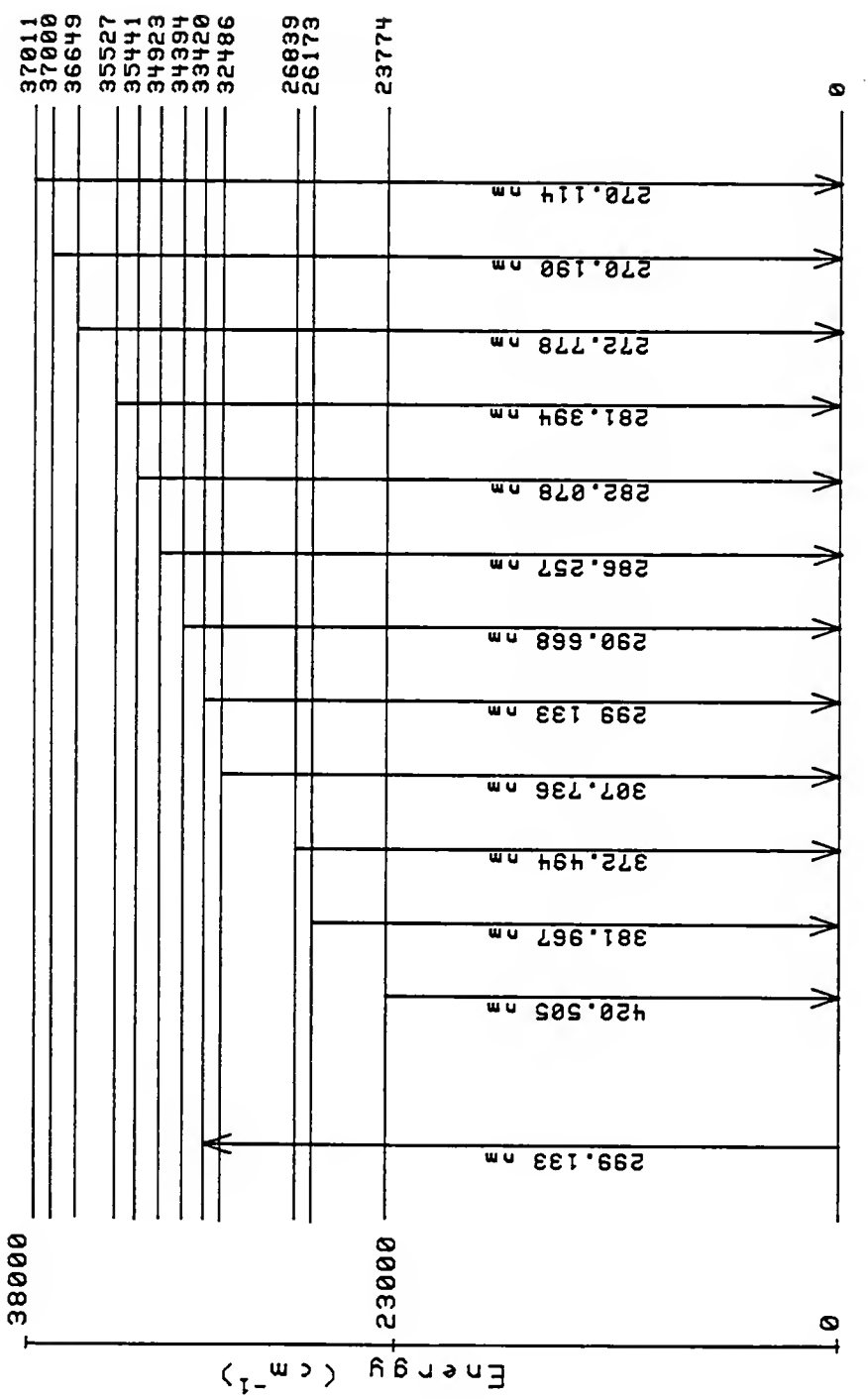

Figure 22. Partial energy level diagram of europium ion (one-step excitation). Wavelengths are also indicated in nm and relative intensities in parentheses.

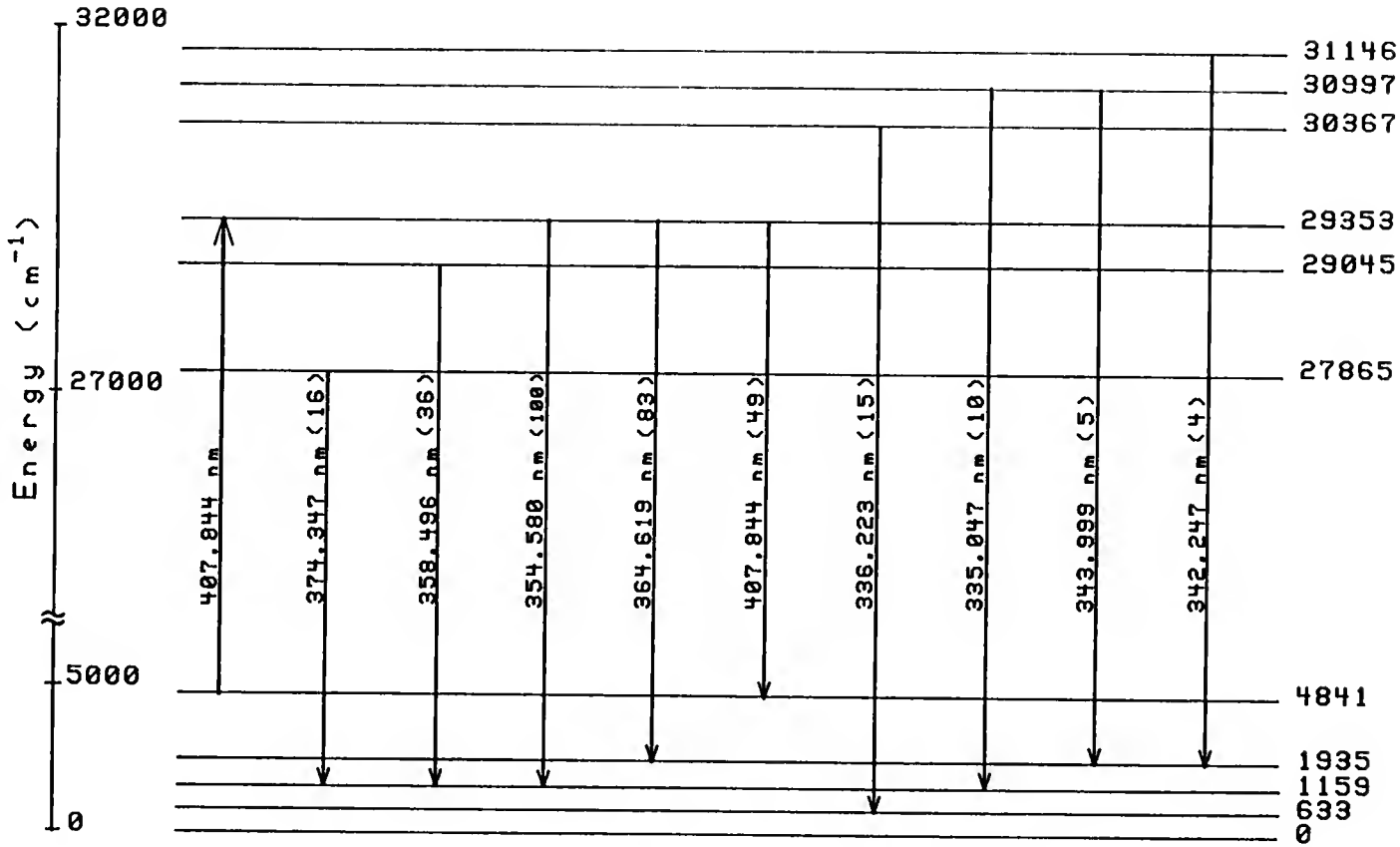

Figure 23. Partial energy level diagram of gadolinium ion (one-step excitation). Wavelengths are also indicated in nm and relative intensities in parentheses.

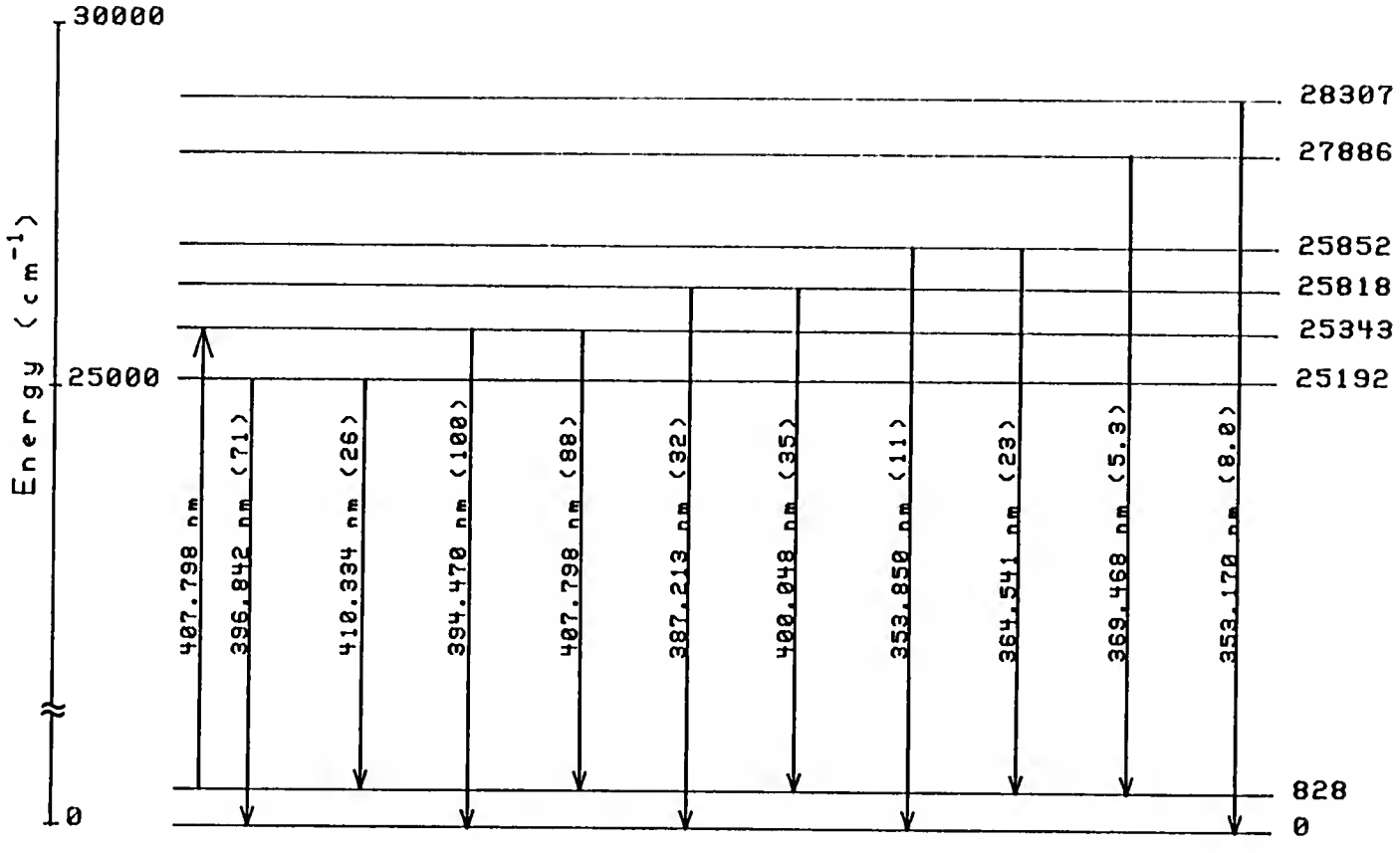

Figure 24. Partial energy level diagram of dysprosium ion (one-step excitation). Wavelengths are also indicated in nm and relative intensities in parentheses.

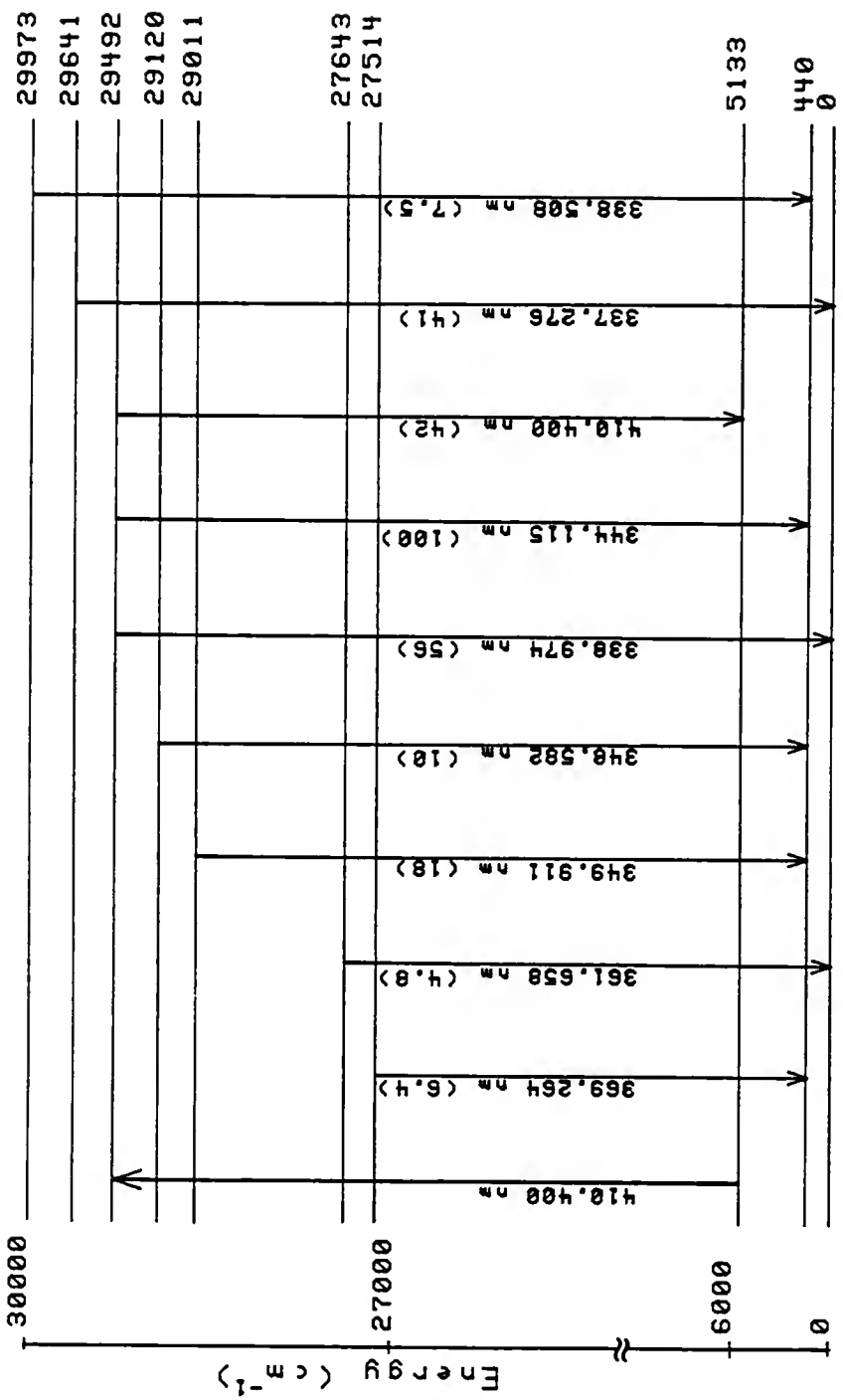

Figure 25. Partial energy level diagram of erbium ion (one-step excitation). Wavelengths are also indicated in nm and relative intensities in parentheses.

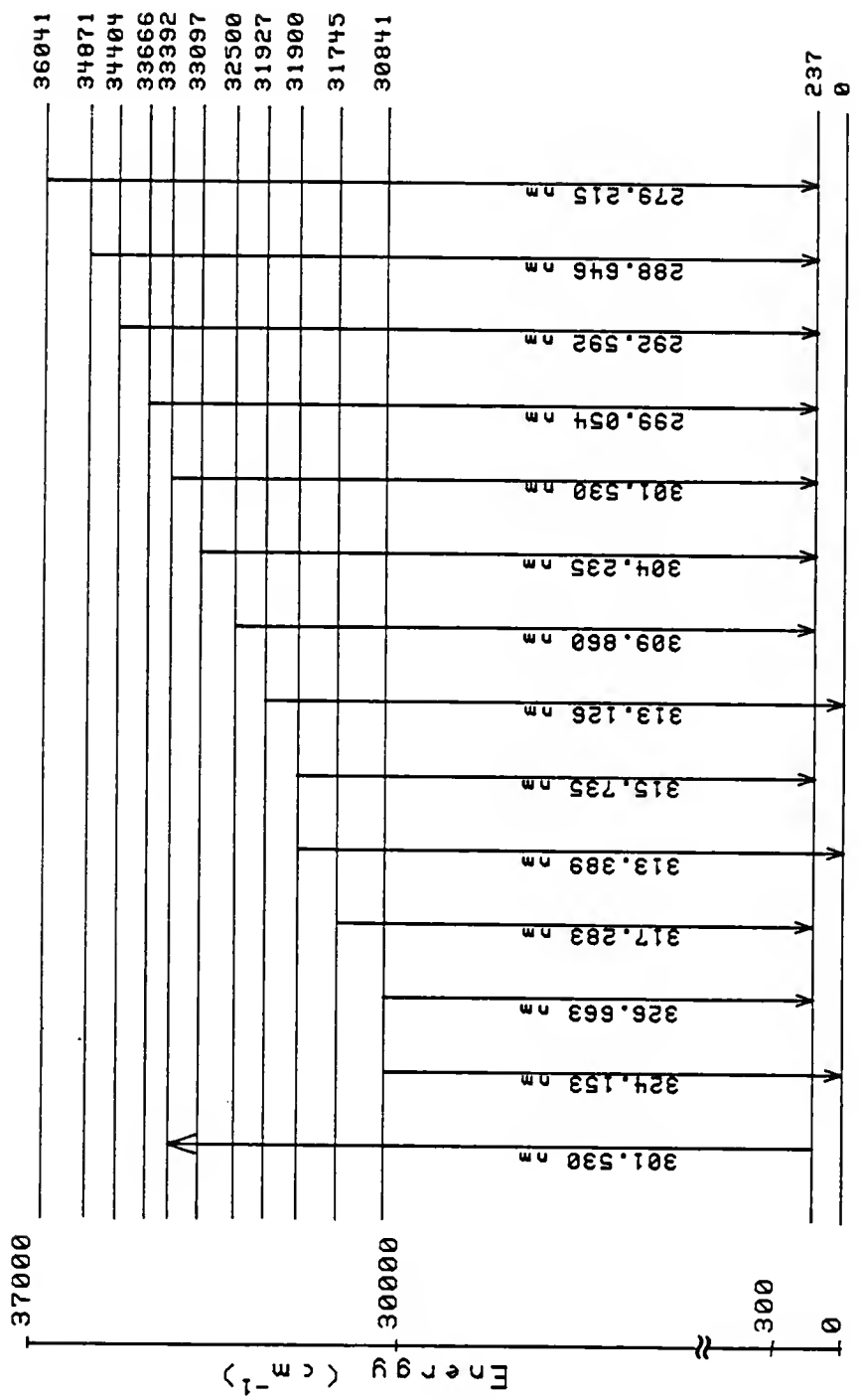

Figure 26. Partial energy level diagram of thulium ion (one-step excitation). Wavelengths are also indicated in nm and relative intensities in parentheses.

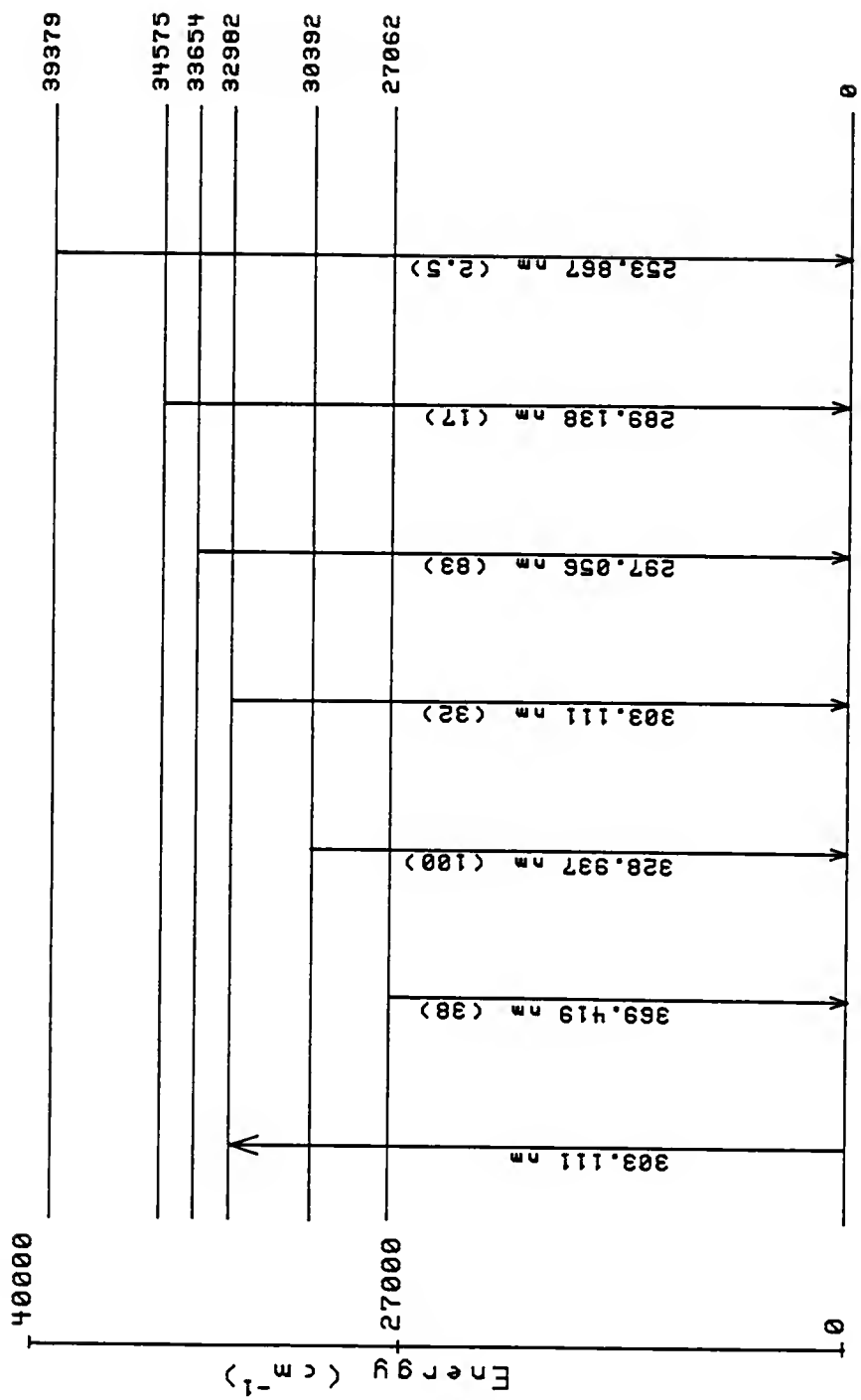

Figure 27. Partial energy level diagram of ytterbium ion (one-step excitation). Wavelengths are also indicated in nm and relative intensities in parentheses.

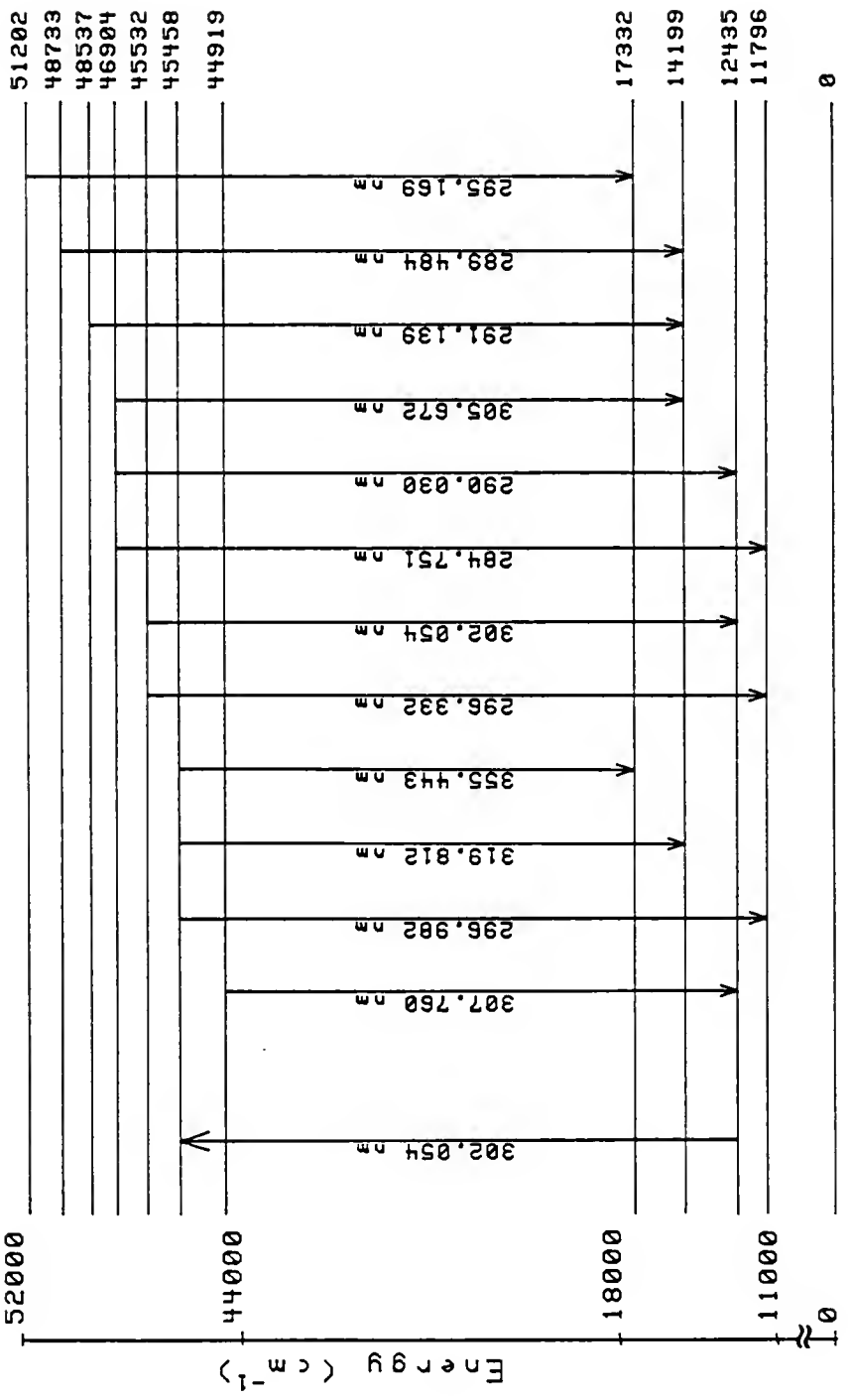

Figure 28. Partial energy level diagram of lutetium ion (one-step excitation). Wavelengths are also indicated in nm and relative intensities in parentheses.

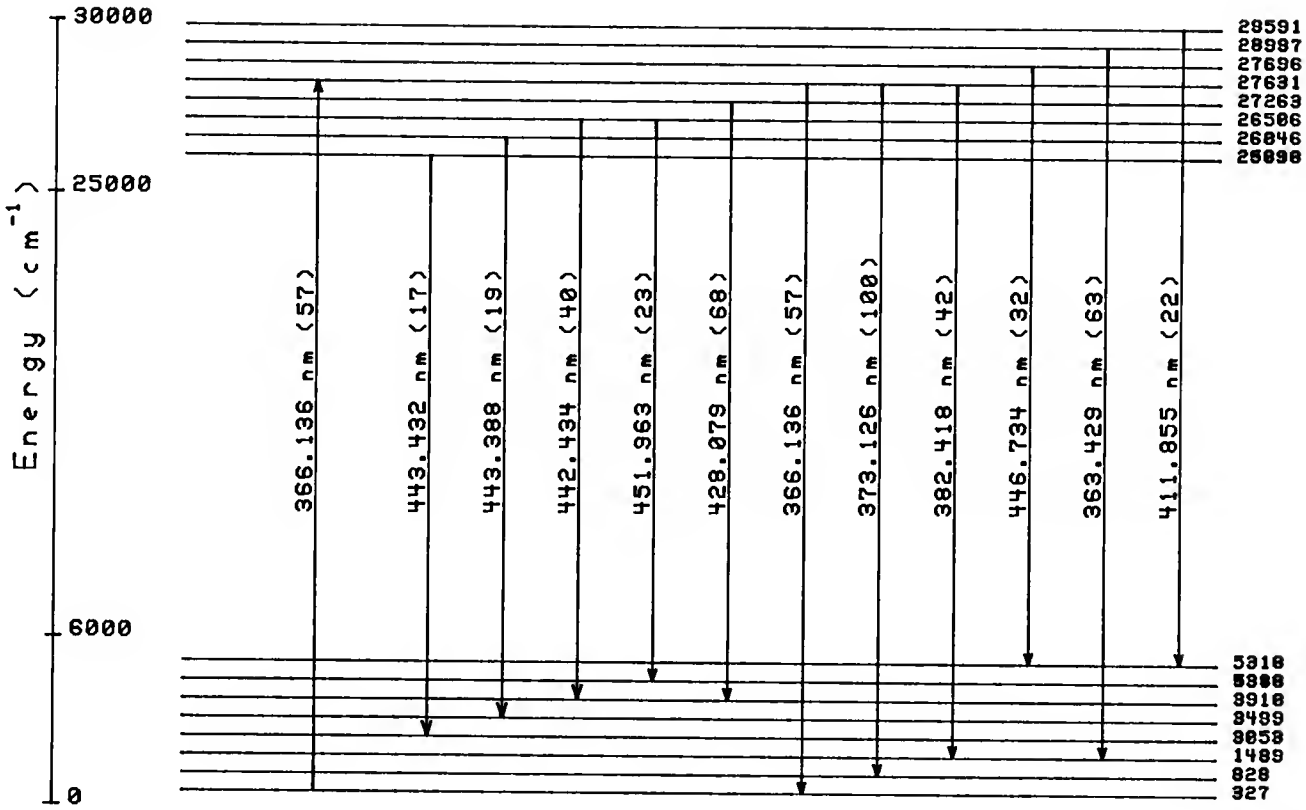

Figure 29. Partial energy level diagram of samarium ion (one-step excitation). Wavelengths are also indicated in nm and relative intensities in parentheses.

in fact be nearly as highly populated as the ground ionic state as a consequence of the high temperature of the ICP.

In most cases, the sensitivity of the S-DLF or AS-DLF exceeds that of the S-SWF or AS-SWF. Even though the DLF signals were usually more intense than the SWF signals, collisional activation-deactivation caused several SWF signals to be intense. As indicated in equation (12), the dominant factor which affects the sensitivity of either DLF or SWF process appeared to be the transition probability of both the excitation and fluorescence line. A second factor which affects the sensitivity of SWF appears to be the energy difference of the upper levels between the laser-excited and fluorescence line. The SWF can be very sensitive when the difference between the upper levels is small. In other words, the degree of mixing between upper levels is greater when the energy difference of the upper levels between the laser-excited and the upper level of the fluorescence transition is small.

The degree of mixing between the laser-excited level and nearby excited levels was examined for dysprosium. The laser excitation at 407.798 nm corresponds to a transition from 828 to 25343 cm^{-1}. The fluorescence signal from upper level 25818 cm^{-1} to the ground ionic state was three times higher than from upper level

28252 cm^{-1} to the ground ionic state. Since the gA values for the two fluorescence transitions are identical ($3.7x10^8$ sec^{-1}), this will not be a significant factor in the relative fluorescence intensities of these two transitions. The only explanation for these two transitions to have different fluorescence intensities should be that the thermally assisted collisional process which occurred after primary excitation was higher for one level than the other. This thermally assisted collisional process is often referred to as mixing between two levels. Therefore, as expected, the degree of mixing between levels 23543 and 25818 cm^{-1} must be three times higher than for levels 23543 and 28252 cm^{-1}.

In all cases when the fundamental dye laser wavelength was used to excite the fluorescence, the pumped transition did not appear to be optically saturated, i.e., decreasing the laser power by a factor of 2 resulted in a decrease of the nonresonance fluorescence signal by a factor of 2. Therefore, the fluorescence signal is dependent upon laser fluctuations.

The precision (%RSD) of the technique at low concentrations is approximately 5%. This is determined by measuring the relative standard deviation (RSD) of 1000 data points at a concentration 10 times greater than the detection limit. At concentrations much greater than the detection limit, the %RSD is approximately 3%.

Conclusion

The detection limits obtained by laser-excited ionic fluorescence spectrometry should be adequate for trace analysis (<1 μg mL^{-1}) of any RE in a complex mixture of all other REs (100 μg mL^{-1}) without spectral interferences. This technique did not require isolation of any of the REs by the use of ion exchange columns or any form of chemical separation which would most likely be required for ICP-ES because of severe spectral interferences.

Upon consideration of the relative fluorescence intensities obtained in Figures 5-17 and according to equation (12), the two most important factors which affect the intensity of ionic fluorescence are the spectral irradiance of the laser and the transition probability value gA. Of course the population density of ions in the lower level from which the absorption process is initiated is also important. A second pass of the laser beam through the plasma was advantageous since it was proven that optical saturation had not been reached.

The laser-ICP system was effective for avoiding spectral interferences observed in ICP-ES. The spectral selectivity offered by this method as well as the tunability of the dye laser makes laser-excited ionic fluorescence spectrometry a potentially useful method for

the analysis of REs in mixtures when high sensitivity, low detection limits and high selectivity are desired.

CHAPTER V
ANALYTICAL STUDIES OF LASER-EXCITED IONIC FLUORESCENCE (TWO-STEP)

Introduction

The goal of this study was to investigate the fluorescence signal obtained when a second laser is introduced into the analytical system. The fluorescence signal using two-step excitation is compared to the fluorescence signal using single-step excitation.

Two-step excitation offers the possibility of populating high lying atomic and ionic levels which usually possess more intense fluorescence characteristics. The ability to populate high lying atomic and ionic levels by two-step excitation is obvious. The use of two-step excitation can shift the wavelength requirement of the pump from the low ultraviolet region to wavelengths typically greater than 300 nm where tunable radiation is easily achieved. The high lying atomic and ionic levels usually possess more intense fluorescence characteristics because it is indicated in equation (12) that the fluorescence radiance is proportional to the frequency of emission ν_{32}. The fluorescence resulting from the two-step excitation can be used for analytical purposes in a similar way that was done for only one laser excitation.

Direct two-photon excited fluorescence using a single wavelength and proceeding through a virtual intermediate level, as shown in Figure 30a, have been observed (65-66). However, the increase in sensitivity resulting from the higher level of excitation achieved is offset by the low probability of such transitions. This process will not be considered in this study.

By using two tunable dye lasers operating at two different wavelengths, much higher sensitivity can be obtained since a real intermediate level can be used rather than a virtual level (see Figure 30b). For this two-step excitation process, the advantage of high excitation energy is maintained and the transition probability is much greater than for two-photon excitation through a virtual level. Since the two excitation transitions share a common level, temporal and spatial coincidence must be assured in the plasma. Furthermore, optically accessible excited electronic states usually have short radiative lifetimes. In order to build up a large enough concentration of the real intermediate level in the two-step excitation scheme, the rate of pumping must be large enough to overcome the radiative losses. The use of pulsed tunable dye lasers should provide high enough pumping rates to apply this technique to the measurement of atomic or ionic species in the plasma.

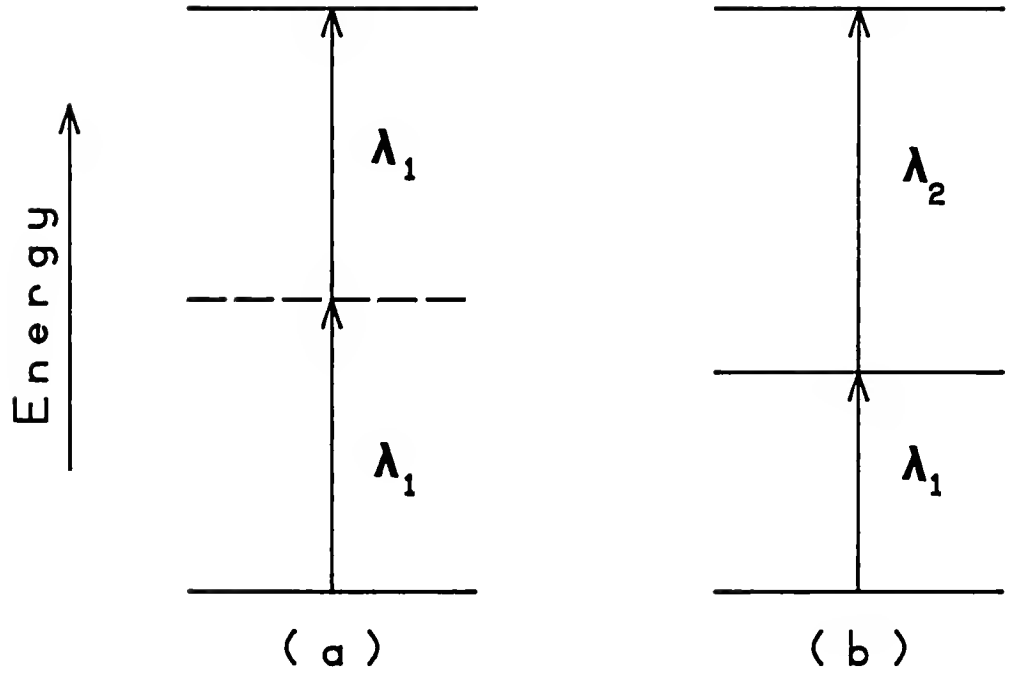

Figure 30. Multiphoton processes: (a) two-photon, single wavelength via a virtual intermediate level; (b) two-step excitation.

Two-step excited fluorescence techniques have not received much attention in the analytical literature (67-69). Since there have been only a few studies performed with the two-step excitation of fluorescence, it appeared reasonable to explore this technique for the measurements of REs in the ICP. Thus, one-step excitation will be compared with two-step excitation.

Experimental

A block diagram of the experimental set-up is shown in Figure 31. Two-step photoexcitation was achieved by using two separately tunable dye lasers pumped with a single excimer laser. The output of the excimer laser was split between the two dye lasers using a 50% dichroic beam splitter. Except for the addition of the second dye laser (Molectron Corporation, Sunnyvale, California, Model DL-II) and the necessary optics, this system was similar to the one described in the previous chapter. The two dye laser beams were directed into the plasma from opposite directions. Mirrors were adjusted to provide maximum spatial overlap of the two beams.

In order to achieve temporal coincidence of the two laser pulses, one laser pulse was delayed with respect to the other by sliding a retroreflector along an optical rail. Temporal coincidence of the two laser beams was then assured by examining their respective temporal

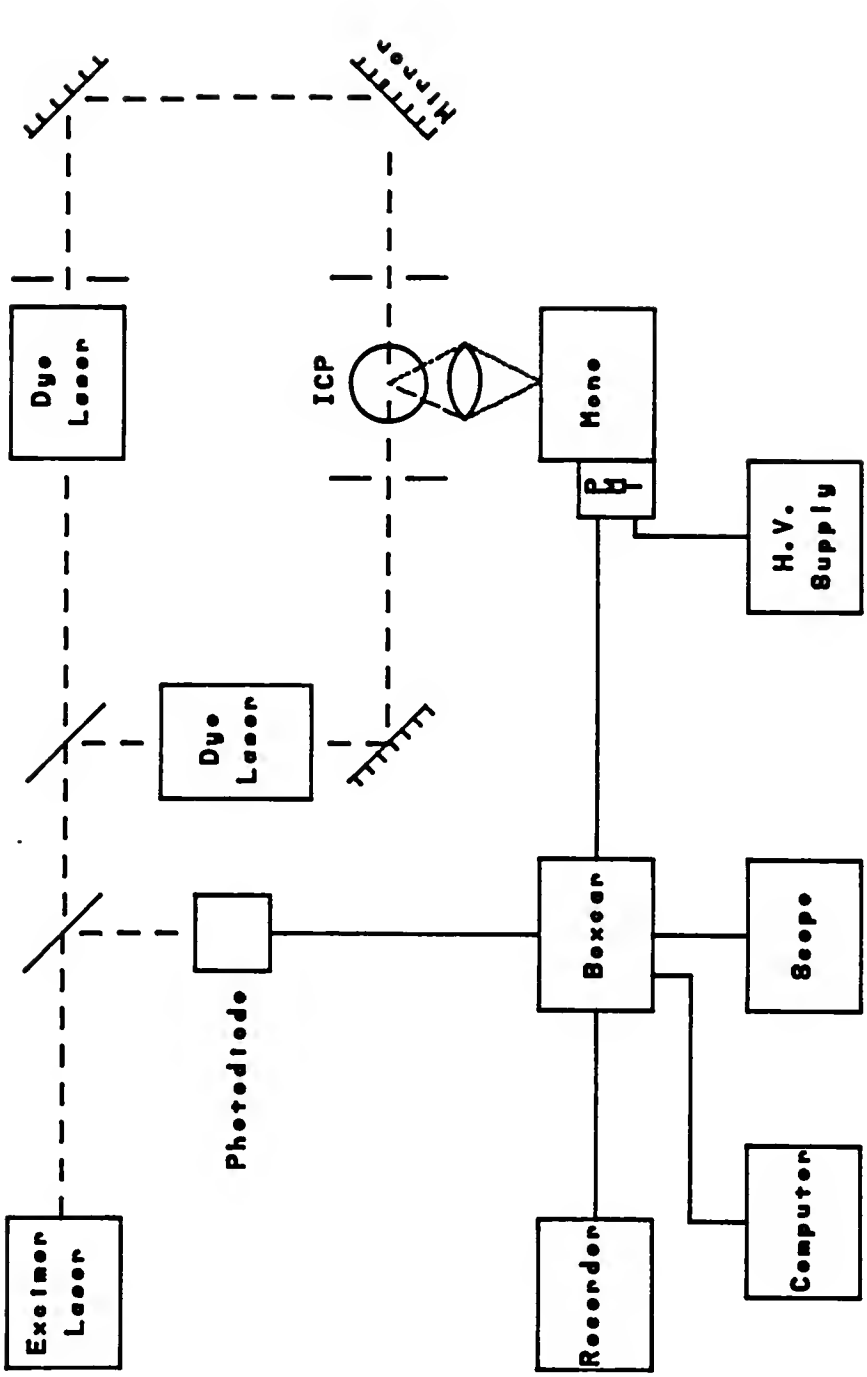

Figure 31. Block diagram of experimental system for laser-excited ionic fluorescence of the rare earth elements in the inductively coupled plasma (two-step excitation).

positions with a fast photodiode (Silicon Photoconductive Detectors, EG&G Electro-Optics, Salem, Mass., model no. FND-100Q) and an oscilloscope (Tektronics, model 2465). The spatial coincidence of the two beams was achieved by a visual alignment over the ICP torch and then by maximizing the signal obtained by the scattering of each laser when water was aspirated through the capillary. Both laser beams were reduced to approximately 3 mm in diameter upon entering the plasma by using apertures.

The output of one dye laser was used to generate the first resonant frequency, λ_1, and the output of the other dye laser was used to generate the second resonant frequency, λ_2. Fluorescence transitions were measured using the same detection system as was used for one-step excitation study. The various laser dyes used for two-step excitation of REs included coumarin 440 and 481 and rhodamine 590, 610 and 640. The concentration and solvents used were those recommended by the Exciton Laser Dye catalog (Exciton Chemical Company, Inc., Dayton, Ohio).

Results and Discussion

In two-step laser-excited ionic fluorescence (LEIF), either of the two wavelengths can be scanned in order to obtain a fluorescence signal. In practice, it was much simpler to start by setting the first excitation

Table 2. Fluorescence transitions and detection limits for the rare earth elements in the inductively coupled plasma (two-step excitation).

Rare Earth Element	First Excitation Wavelength (Transition, cm^{-1})[a] ℓ --> u_1	Second Excitation Wavelength (Transition, cm^{-1})[a] u_1 --> u_2	Flourescence Wavelength (nm) (Transition, cm^{-1})[a] u_2 --> ℓ	Detection Limit
La	457.488 (1394 - 23247)	618.809 (23247 - 39403)	421.756 (39403 - 15699)	240
Eu	443.556 (1669 - 24208)	306.911 (24208 - 56781)	333.875 (56781 - 26838)	250
Yb	289.138 (0 - 34575)	506.731 (34575 - 54304)	366.970 (54304 - 27062)	170
Lu	646.312 (11796 - 27264)	571.349 (29407 - 46904)	290.030 (46904 - 12435)	1800

[a] Energy levels in cm^{-1}; ℓ = lower level; u_1 = upper level of first laser excitation; u_2 = upper level of second laser excitation.

wavelength by monitoring one of its nonresonance fluorescence transition. Once this transition was determined, the second laser was scanned. It was also much easier to find excitation transitions which did not require the use of frequency doubling in order to avoid the difficulty of tracking the angle-tune double crystal with the wavelength of the dye laser.

Analytical calibration curves were constructed for the two-step LEIF of lanthanum, europium, ytterbium and lutetium and are given in Figures 32-35. One can see that, as expected, the linearity of this technique is similar to the single-step fluorescence.

No enhancement in the fluorescence signal was achieved when comparing two-step excitation to one-step excitation. In fact, the detection limits using single-step excitation were lower than the ones obtained using two-step excitation. One explanation may be that when the two dye lasers were used, the excimer laser beam had to be split into two beams using a 50% beam splitter. In so doing, only half of the pump laser beam was directed into each dye laser. It was experimentally proven that if intensity of the pump laser was decreased by a factor of 2, the output of the dye laser was decreased by a factor of 4. Therefore, four times less power was available in order to excite the various transitions. Since optical saturation has not been reached, the signal-to-noise ratio

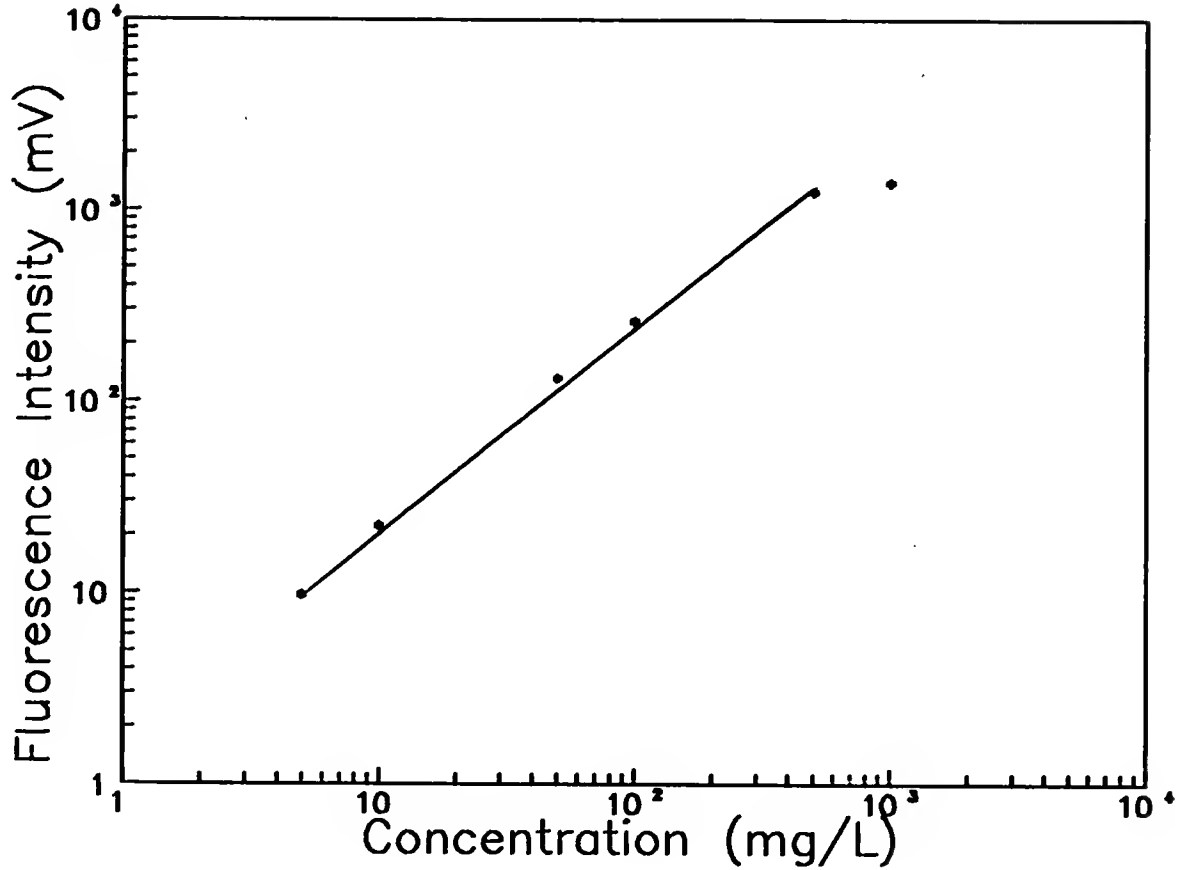

Figure 32. Analytical calibration curve for ionic fluorescence of lanthanum (excitation at 457.488 nm and 618.809 nm and detection at 421.756 nm).

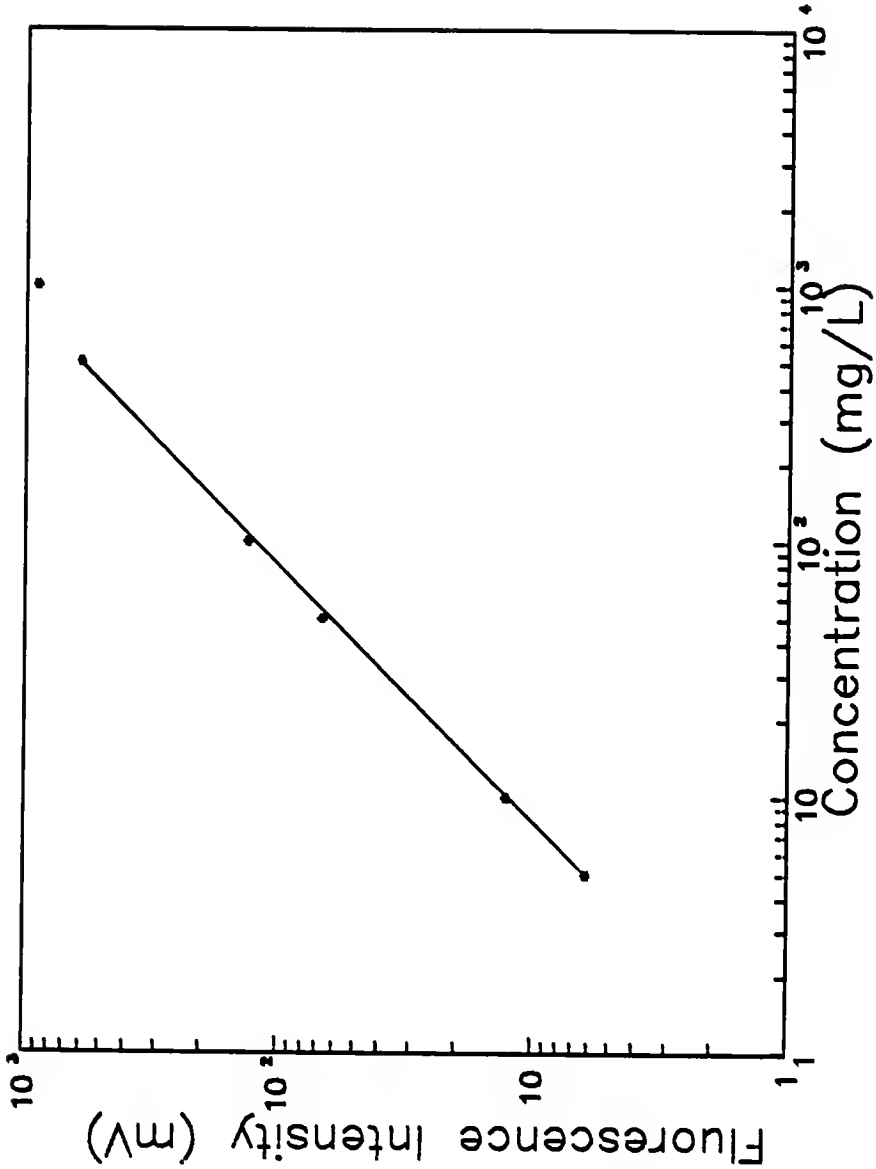

Figure 33. Analytical calibration curve for ionic fluorescence of europium (excitation at 443.556 nm and 306.911 nm and detection at 333.875 nm).

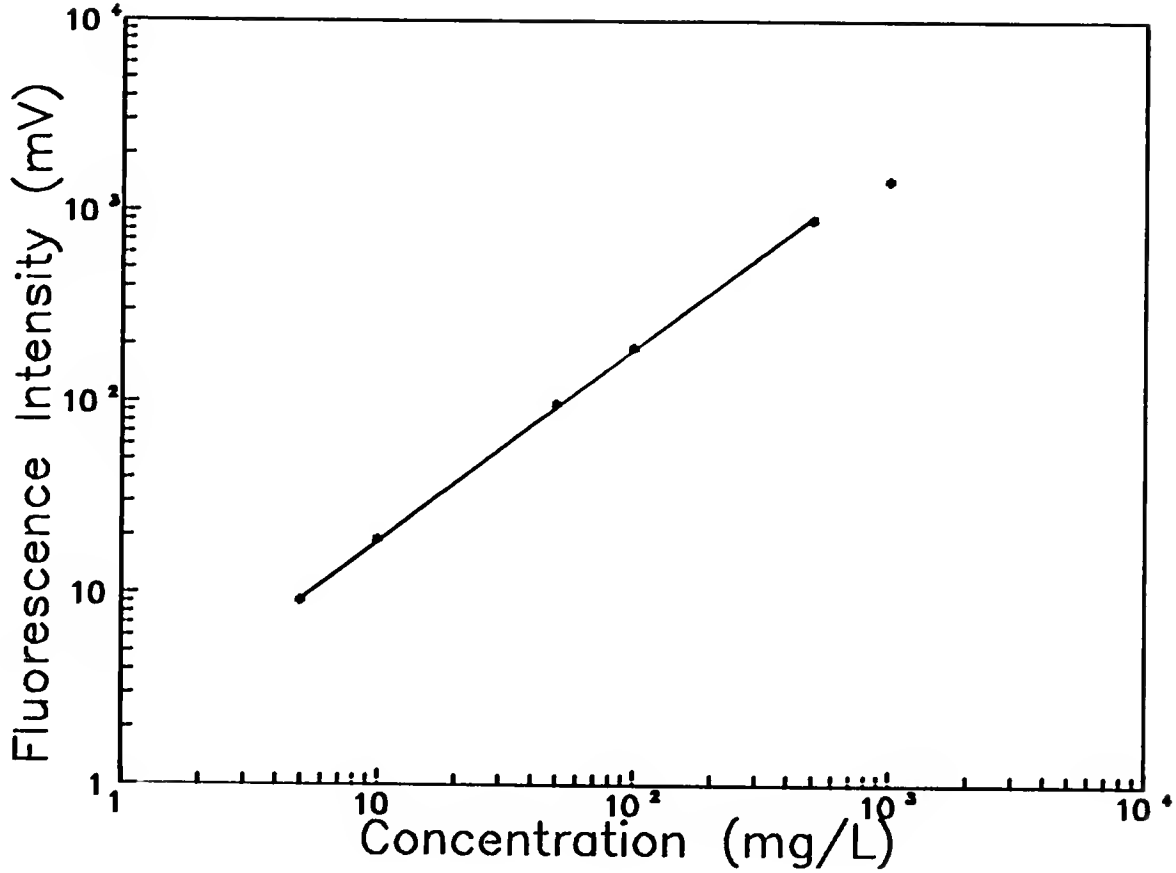

Figure 34. Analytical calibration curve for ionic fluorescence of ytterbium (excitation at 289.139 nm and 506.731 nm and detection at 366.970 nm).

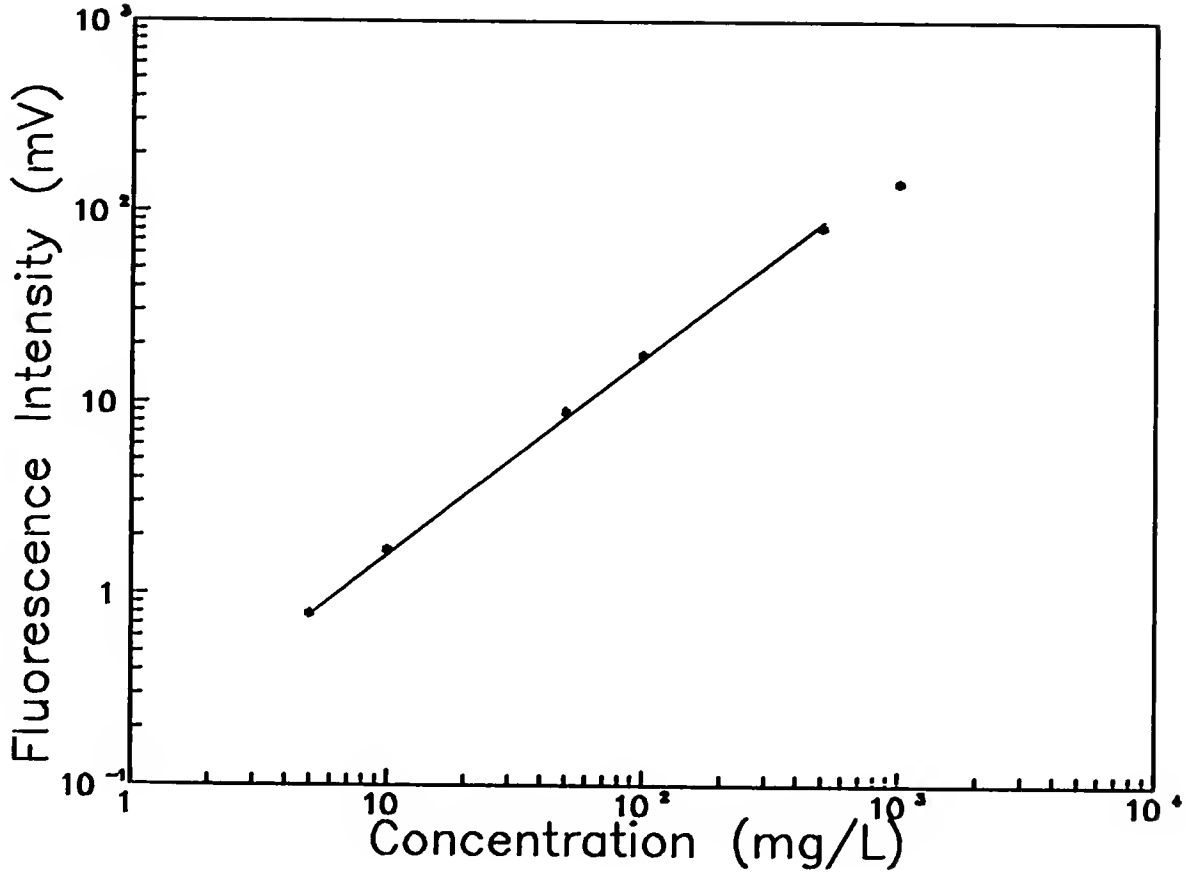

Figure 35. Analytical calibration curve for ionic fluorescence of lutetium (excitation at 646.312 nm and 571.349 nm and detection at 290.030 nm).

and thus the detection limits would improve by increasing the output of power of the dye lasers.

Partial energy level diagrams were constructed for the two-step excitation of lanthanum, europium, ytterbium and lutetium (Figures 36-39). As shown in Figure 36, the first laser provided the excitation of lanthanum ions from 1394 cm^{-1} to 23247 cm^{-1}. The second laser then provided the excitation of the ions from 23247 cm^{-1} to 40458 cm^{-1}, and the fluorescence was monitored at several wavelengths. In most studies concerning two-step excitation, the level reached by the first laser is the starting level of the second excitation transition. However, as shown in Figure 37, the two-step excitation scheme can be used even when the two excitation transitions do not share a common level. This scheme was only applied to lutetium ions but it could be extended to other REs. As indicated by the higher detection limits, the lower level of the second excitation which was indirectly coupled is probably not as populated as if it had been directly coupled.

Conclusion

The two-step fluorescence technique permits direct access to highly excited levels whose thermal population is low even at the elevated temperature of the ICP. It is, therefore, expected that the emission signal, which in

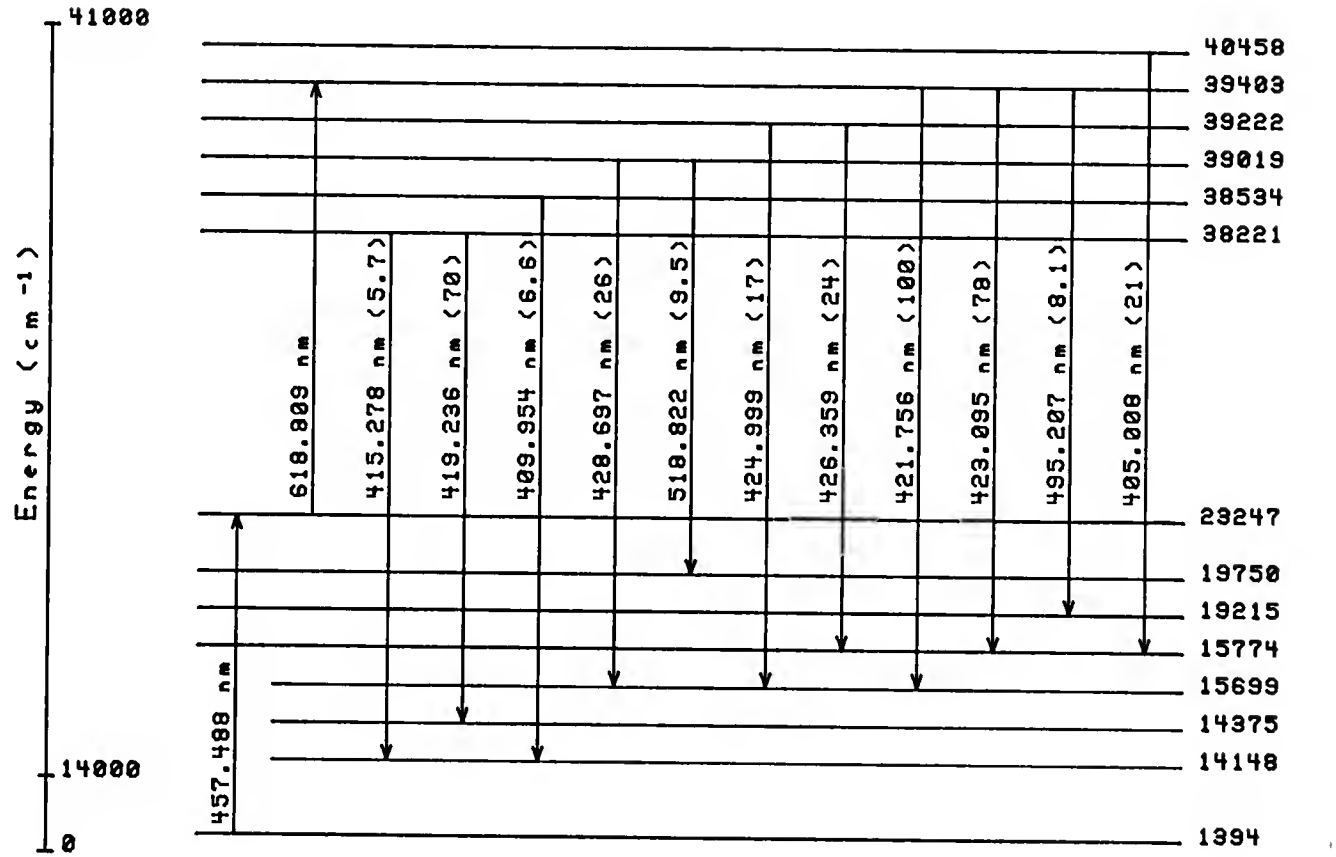

Figure 36. Partial energy level diagram of lanthanum ion (two-step excitation). Wavelengths are also indicated in nm and relative intensities in parentheses.

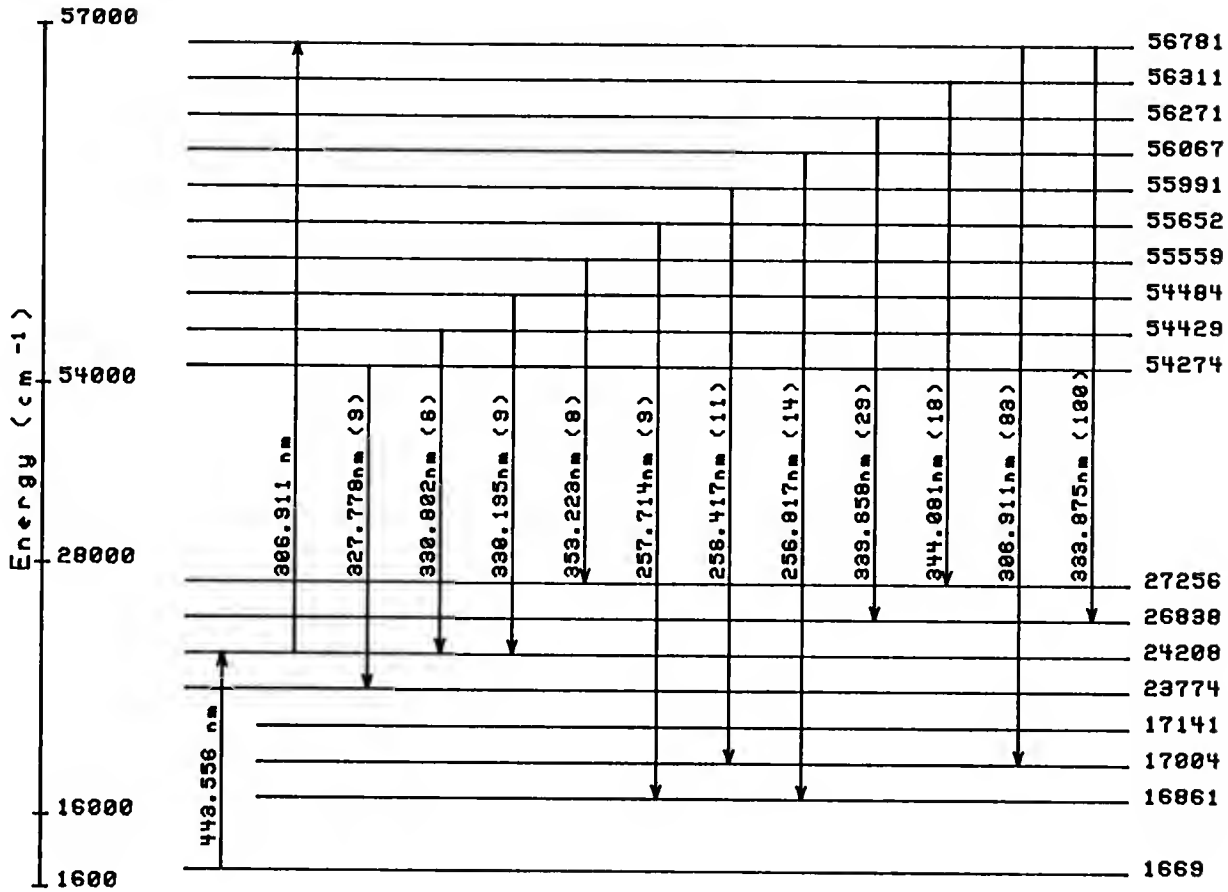

Figure 37. Partial energy level diagram of europium ion (two-step excitation). Wavelengths are also indicated in nm and relative intensities in parentheses.

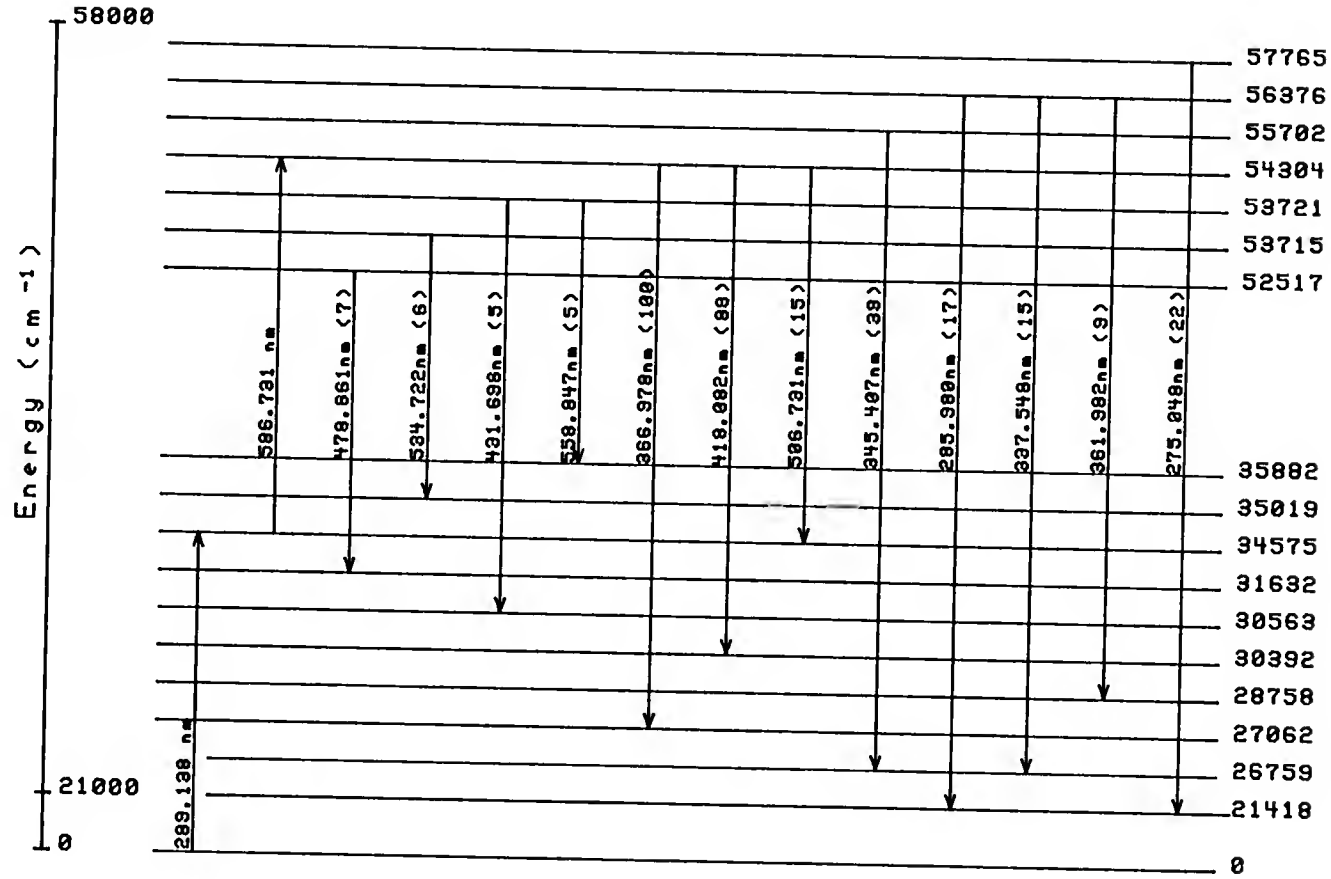

Figure 38. Partial energy level diagram of ytterbium ion (two-step excitation). Wavelengths are also indicated in nm and relative intensities in parentheses.

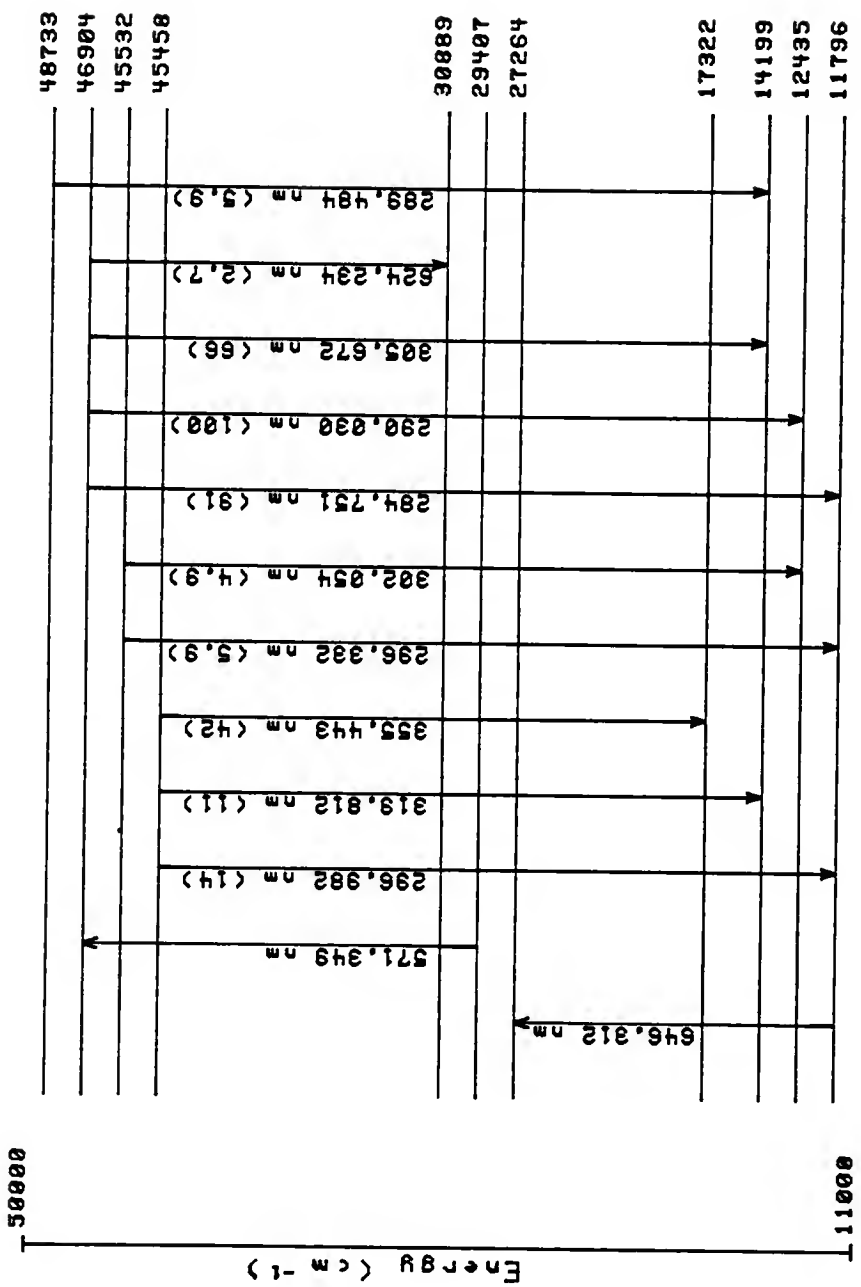

Figure 39. Partial energy level diagram of lutetium ion (two-step excitation). Wavelengths are also indicated in nm and relative intensities in parentheses.

this case is a source of noise, would be less and thus the signal-to-noise ratio would improve. The emission signal for one-step excitation is expected to be higher than for two-step excitation because the thermal population of the levels which can be reached by only one laser becomes more significant. Therefore, the advantage of exciting the ions to a higher energy level is mostly a decrease in the background emission noise from the ICP.

It was shown in the Results and Discussion section that the spectral irradiance of the lasers for the two-step excitation process is approximately four times less than the spectral irradiance of the laser used for one-step excitation. Therefore, the fluorescence radiance is expected to be four times less, and thus the detection limits for the two-step process should be four times higher than for the one-step process. However, the results obtained indicated that the detection limits for one or two lasers are similar. Since the gA values for the excitation and fluorescence processes of the one-step and two-step technique were similar, the background noise must have been less for the two-step process than for the one-step process.

Since it is possible that two elements may be excited at the same wavelength with only one laser, the addition of a second laser offers the advantage of increased selectivity. In other words, the probability of a

contaminant being excited by both dye laser wavelengths is greatly reduced.

Even though sustained enhancement of the detection limit was not achieved using two-step excitation as compared to one-step excitation, this technique may become important as a tool for the study of the excitation dynamics in plasmas. However, it is predicted that the detection limits measured using two lasers could be improved by increasing the output power of the pump laser.

The use of single-step or two-step LEIF minimizes some of the severe interference problems which occur by ICP-ES. A common problem which was eliminated was the overlap of spectral lines of the various elements present in the sample. The analytical results obtained for single-step and two-step LEIF of the REs in the ICP have indicated that it may be the method of choice for the analysis of REs in a mixture when high sensitivity as well as very high selectivity are desired.

CHAPTER VI
FUTURE WORK--IMPROVEMENTS

Future studies which should provide some improvements in the detection limits obtained by one- or two-step laser excitation of ionic fluorescence of REs in the ICP include the use of lasers which possess more power. For example, the output energy of a dye laser pumped with a Nd:YAG laser using Rhodamine 6G can approach 50 to 100 mJ per pulses. However, the output energy of the dye laser used for this thesis work was approximately 3 mJ per pulses for the same laser dye.

Furthermore, it would be interesting to try to use a high intensity continuum source such as a pulsed xenon flashlamp in order to investigate both one- and two-step excitation of REs in the ICP. The estimated output energy of a pulsed xenon flashlamp source over the absorption linewidth of an atom or ion should approach 1 mJ. It will also be interesting to find out the results of Demers and Shrabak (8) for excitation of atoms and ions in the ICP using the new boosted-output HCLs which are discussed in the introduction.

Another method which would facilitate detection and also give much more information for various excitation

wavelengths is to replace the photomultiplier tube with an intensified photodiode array (IPDA). Upon using two-step excitation in order to populate high lying ionic levels and using an IPDA as a detector, it would be possible to identify several unclassified RE transitions. Future studies should also investigate the analysis of real samples, especially those containing complex matrices of multiple REs.

REFERENCES

1. E.L. Nichols and H.L. Howes, Phys. Rev. 23, 472 (1924).

2. J.D. Winefordner and T.J. Vickers, Anal. Chem. 36, 161 (1964).

3. J.D. Winefordner, V. Svoboda and L.J. Cline, CRC Critical Reviews in Analytical Chemistry 1, 233 (1970).

4. R.M. Dagnall and T.S. West, Appl. Opt. 7, 1287 (1968).

5. N. Omenetto and J.D. Winefordner, Prog. Anal. At. Spetrosc. 2, 1 (1979).

6. J.D. Winefordner and R.A. Staab, Anal. Chem. 36, 165 (1964).

7. D.N. Armentrout, Anal. Chem. 38, 1235 (1966).

8. D.R. Demers and J.W. Skrabak, Presented at Colloquium Spectroscopicum Internationale, June 21-26, 1987, Toronto, Canada, abstract number F8.4.

9. C. Veillon, J.M. Mansfield, M.L. Parsons and J.D. Winefordner, Anal. Chem. 38, 204 (1966).

10. R.M. Dagnall, T.S. West and P. Young, Talanta 13, 803 (1966).

11. D.H. Burling, M. Czajouski and L. Krause, J. Opt. Soc. Amer. 57, 1162 (1967).

12. R.M. Dagnall, K.C. Thompson and T.S. West, Talanta 14, 1467-1475 (1967).

13. M.S. Epstein, N. Omenetto, S. Nikdel, J. Bradshaw and J.D. Winefordner, Anal. Chem. 52, 284 (1980).

14. L.M. Fraser and J.D. Winefordner, Anal. Chem. 43, 1693 (1971).

15. M.B. Denton and H.V. Malmstadt, Appl. Physics Letters 18, 485 (1975).

16. N. Omenetto and H. G. C. Human, Spectrochim. Acta 39B, 1333 (1984).

17. I.M. Fraser and J.D. Winefordner, Anal. Chem. 44, 1444 (1972).

18. H.L. Brad and E.S. Yeung, Anal. Chem. 48, 344 (1976).

19. M.S. Epstein, J. Bradshaw, S. Bayer, J. Bower, E. Voigtman and J.D. Winefordner, Appl. Spect. 34, 372 (1980).

20. J.J. Horvath, J.D. Bradshaw, J.N. Bower, M.S. Epstein and J.D. Winefordner, Anal. Chem. 53, 6 (1981).

21. S.J. Weeks, H. Hapacuchi and J.D. Winefordner, Anal. Chem. 50, 360 (1978).

22. N. Omenetto, N.N. Hatch, L.M. Fraser and J.D. Winefordner, Spectrochim. Acta 28B, 65 (1973).

23. M.A. Bolshov, A.V. Zybin, V.G. Koloshnikov and M.V. Vasnetsov, Spectrochim. Acta 36B, 345 (1981).

24. K. Dittrich and H. Stark, J. Anal. At. Spectrom. 1, 237 (1986).

25. D. Goforth and J.D. Winefordner, Anal. Chem. 58, 2598, (1986).

26. V.A. Fassel, Anal. Chem. 51, 1290A (1970).

27. H.G.C. Human, N. Omenetto, P. Cavalli and G. Rossi, Spectrochim. Acta 39B, 1345 (1984).

28. B.D. Pollard, M.B. Blackburn, S. Nikdel, A. Massoumi and J.D. Winefordner, Appl. Spectrosc. 33, 5 (1979).

29. A. Montaser and V.A. Fassel, Anal. Chem. 48, 1490 (1976).

30. M.A. Kosinski, H. Uchida and J.D. Winefordner, Talanta 30, 339 (1983).

31. N. Omenetto, S. Nikdel, R.D. Reeves, J.B. Bradshaw, J.N. Bower and J.D. Winefordner, Spectrochim. Acta 35B, 507 (1980).

32. H. Uchida, M.A. Kosinski and J.D. Winefordner, Spectrochim. Acta 38B, 1345 (1983).

33. M.S. Epstein, S. Nikdel, J.D. Bradshaw, M.A. Kosinski, J.N. Bower and J.D. Winefordner, Anal. Chim. Acta 113, 22 (1980).

34. H.P. Hooymayers, Spectrochim. Acta 23B, 567 (1968).

35. N. Omenetto, F. Benetti, L.P. Hart, J.D. Winefordner and C.T. Alkemade, Spectrochim. Acta 28B, 289 (1973).

36. G.D. Boutilier, M.B. Blackburn, J.M. Mermet, S.J. Weeks, H. Haragushi, J.D. Winefordner and N. Omenetto, Appl. Opt. 17, 2291 (1978).

37. J.W. Daily, Appl. Opt. 15, 955 (1976).

38. B.J. Jansen and T. Hollander, Spectrochim. Acta 32B, 165 (1977).

39. D.R. Olivares and G.M. Hieftje, Spectrochim. Acta 33B, 79 (1978).

40. N. Omenetto, Analytical Laser Spectroscopy, J. Wiley & Sons Ltd., New York (1979).

41. N. Omenetto, L.P. Hart, P. Benetti and J.D. Winefordner, Spectrochim. Acta 28B, 301 (1973).

42. N. Omenetto, J.P. Winefordner and C.T.J. Alkemade, Spectrochim. Acta 30B, 335 (1975).

43. J.D. Winefordner, J. Chem. Ed. 55, 72 (1978).

44. D.R. Olivares and G.M. Hieftje, Spectrochim. Acta 33B, 79 (1978).

45. J.C. Van Loon, Anal. Chem. 53, 333A (1981).

46. N. Omenetto, J.D. Winefordner, "Atomic Fluorescence Spectroscopy with Laser Excitation" in Analytical Laser Spectroscopy, P.J. Elving and J.D. Winefordner, Eds., Wiley, New York (1979).

47. P.J. Zeegers and J.D. Winefordner, Spectrochim. Acta 26B, 161 (1971).

48. N. Omenetto and J.D. Winefordner, Appl. Spectrosc. 26, 555 (1972).

49. G.E. Gordon, K. Randle, G.G. Coles, M.H. Beeson and S.S. Oxley, Geochim. Cosmochim. Acta 32, 369 (1968).

50. P. Voldet and W. Haerdi, Anal. Chim. Acta 97, 185 (1978).

51. M. Thirlwall, Chem. Geol. 35, 155 (1981).

52. C.H. Corliss and W.R. Bozman, NBS Monograph 53 (1963).

53. L.A. Ovchar and N.S. Poluektov, Zh. Anal. Khim. 22, 45 (1967).

54. R.N. Kniseley, C.C. Bottler and V.A. Fassel, Anal. Chem. 41, 1494 (1969).

55. J.G. Crock and F.E. Lythe, Anal. Chem. 54, 1329 (1982).

56. A. Bolton, J. Hwang and A.V. Bolt, Spectrochim. Acta 38B, 165 (1983).

57. S. Nikdel, A. Massoumi and J.D. Winefordner, Microchem. J. 24, 1 (1979).

58. R.K. Winge, V.J. Peterson and V.A. Fassel, Appl. Spectrosc. 33, 206 (1979).

59. R.S. Houk, V.A. Fassel, G.D. Flesch, H.J. Svec, A.L. Gray and C.E. Taylor, Anal. Chem. 52, 2283 (1980).

60. E.C. Subbarao and W.E. Wallace, Science and Technology of Rare Earth Materials, Academic Press, New York (1980).

61. L. Eyring, Progress in the Science and Technology of the Rare Earths, The Macmillan Company, New York (1964).

62. C.A. Hampel, Glass Ind. 41, 82 (1960).

63. G.J. McCarthy and J.J. Rhyne, The Rare Earths in Modern Science and Technology, Plenum Press, New York (1977).

64. M.L. Parsons, B.W. Smith and G.E. Benttley, Handbook of Flame Spectroscopy, Plenum Press, New York (1975).

65. G.C. Turk, J.C. Travis, J.R. DeVoe and T.C. O'Haver, Anal. Chem. 50, 817 (1978).

66. J.C. Travis, P.K. Schenck, G.C. Turk and W.G. Mallard, Anal. Chem. 51, 1516 (1979).

67. A.W. Miziolek and R.J. Willis, Opt. Lett. 6, 528 (1981).

68. J.E.M. Goldsmith and R.J.M. Anderson, Opt. Lett. 24, 607 (1985).

69. N. Omenetto, B.W. Smith and L.P. Hart, Fresenius Z. Anal. Chem. 324, 683 (1986).

APPENDIX
GLOSSARY OF ACRONYMS

AFS	atomic fluorescence spectrometry
DLF	direct line fluorescence
EDL	electrodeless discharge lamp
HCL	hollow cathode lamp
ICP	inductively coupled plasma
ICP-ES	inductively coupled plasma emission spectrometry
LEAFS	laser-excited atomic fluorescence spectrometry
LEIF	laser-excited ionic fluorescence
LOD	limit of detection
RE	rare earth
RF	resonance fluorescence
SNR	signal-to-noise ratio
SWF	stepwise fluorescence

BIOGRAPHICAL SKETCH

Mario Elmen Tremblay was born on October 6, 1960, in Laval, Quebec, Canada. He attended Polyvalente A.N. Morin in Mont Rolland, Quebec, Canada, where he received his high school diploma in 1977.

He then moved to Florida and received his Associate of Art degree from Daytona Beach Community College. Since then, he has attended the University of Florida where he received his Bachelor of Science degree in chemistry in 1983 and his Ph.D. degree in analytical chemistry in 1987 under the supervision of Dr. James D. Winefordner.

I certify that I have read this study and that in my opinion it conforms to acceptable standards of scholarly presentation and is fully adequate, in scope and quality, as a dissertation for the degree of Doctor of Philosophy.

James D. Winefordner, Chairman
Graduate Research Professor of Chemistry

I certify that I have read this study and that in my opinion it conforms to acceptable standards of scholarly presentation and is fully adequate, in scope and quality, as a dissertation for the degree of Doctor of Philosophy.

Gerhard M. Schmid
Associate Professor of Chemistry

I certify that I have read this study and that in my opinion it conforms to acceptable standards of scholarly presentation and is fully adequate, in scope and quality, as a dissertation for the degree of Doctor of Philosophy.

Carol J. Murphy
Associate Professor of Romance Languages and Literatures

This dissertation was submitted to the Graduate Faculty of the Department of Chemistry in the College of Liberal Arts and Sciences and to the Graduate School and was accepted as partial fulfillment of the requirements for the degree of Doctor of Philosophy.

December, 1987

Dean, Graduate School